Politecnico di Torino

Politecnico di Torino

Master's degree in Electronic Engineering
Academic Year 2021/2022
Graduation Session: April 2022

Exact design of an LLC resonant converter for Wireless Power Transfer

Supervisor:
Prof. Gianluca Setti
Co-supervisors:
Prof. Fabio Pareschi
Ing. Andrea Celentano

Author:
Domenico Salime 269570

Contents

Contents

Introduction

The main goal of many power electronics circuits is to ensure transfer of electrical energy with high efficiency and with a good power density, i.e., the ratio between power and volume occupied. Typical converters, based on PWM, cannot achieve high efficiency at high frequency because they work in hard-switching mode. In fact, during switch's transitions there is an overlap between the voltage across the power switch and the current through it, which causes the largest part of converter losses. In many times, these converters are replaced by resonant soft-switching converters. As a matter of fact, these converters are capable of a better efficiency at high frequency since they can avoid the overlap between current and voltage. Thanks to the high operating frequency, they can be designed with smaller reactive elements (mostly inductors) providing a higher power density.

Currently, the LLC is one of the most employed resonant converters. Its name derives from the main circuit topology, which is composed by two inductors (LL) and one capacitor (C). LLC resonant converter can perform power conversion through frequency modulation (instead of PWM), and it can easily achieve high efficiency. Nevertheless, due to the intrinsic nonlinearity and the presence of the three reactive elements (two inductors and a capacitor), the design of LLC resonant converters is not an easy task to be performed. In the literature the vast majority of the publications which refers to LLC resonant converters, bases its design on the so called First Harmonic Approximation (FHA). This is a simplified approach where current and voltage signals in the converter that are sinusoidal-like, are assumed to be purely single sinusoidal tones. The analysis by means of FHA is strongly simplified and introduces strong approximations which cannot be accepted in practice. Furthermore, FHA is not capable to consider any sources of loss due to non-idealities of the circuital elements.

The aim of this thesis regards the design optimization of an LLC resonant converter for Wireless Power Transfer (WPT) by means of a semi-analytical design approach, in which the main sources of losses can be considered. In particular, when the LLC is adopted for WPT, the transformer is replaced with two coupled inductors, which are not well coupled and therefore lead to high leakage inductances. As counteraction, we avoid one inductor of the LLC and exploit the leakage one instead. At the end of this thesis, the exact semi-analytical design is obtained through a switching sequence technique implemented by means of MATLAB scripts. The MATLAB results have been verified to be in agreement with the LTspice simulations. In conclusion, the limits of the LLC converter, when employed for WPT, are highlighted.

1. Wireless Power Transfer

Wireless Power Transfer (WPT) is a technique that has emerged recently with the aim to replace the standard power supply based on wires. There are two main methodologies to do WPT: inductive coupling, based on magnetic field, and capacitive coupling which is based on an electric field. In this work, inductive coupling is taken into account. WPT has many industrial and biomedical applications. One example is the Wireless Health Advanced Monitoring bio-diagnostic system (WHAM-BioS). This is a system embedded in the human body which constantly samples and records the biomedical signals. This circuit needs energy to work and a contactless power transmission, which is a convenient solution to overcome the issues derived from a wire-based system (physical contact) or from implanted batteries (longevity, size).

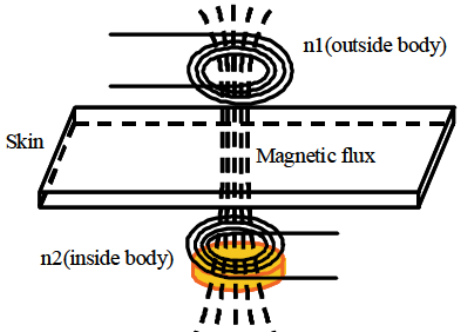

Figure 1. 1: schematic drawing of the coupling coils for WHAM-Bios

1.1 Coupled inductors and coupling coefficient k

A generic transformer is composed of two wires wrapped around a magnetic core which transfers energy directly from primary to secondary winding. In an ideal transformer the coupling between primary and secondary is of 100% and the leakage inductance is zero. A transformer can't store energy. The mutual inductance between two coils (with inductances respectively L_1 and L_2), assuming zero leakage and 100% magnetic coupling, is expressed as:

$$M = \sqrt{L_1 \cdot L_2}\ [H] \qquad (1.1)$$

In coupled inductors the coils are not perfectly coupled since there is not the iron core as in the transformer. Consequently, coupled inductors have consistent leakage inductance and can store energy. The amount of magnetic flux that links the two coils is expressed by the coupling coefficient k, a fractional number between 0 and 1. If k=1, the two coils are completely coupled, which is the case of an ideal transformer. On the other

hand, if k=0 the two coils are not coupled. The expression of the mutual inductance becomes the following:

$$M = k \cdot \sqrt{L_1 \cdot L_2}\ [H] \tag{1.2}$$

The coupling coefficient k can be expressed as:

$$k = \frac{M}{\sqrt{L_1 \cdot L_2}} \tag{1.3}$$

Coupling coefficient k is dependent on the distance between the two inductors and other factors. In fact, k decreases as the distance between the two inductors increases. In Wireless Power Transfer systems, coupled inductors with low values of k are often used, and it is difficult to have a k above 0.6-0.7.

1.2 Equivalent circuit for coupled inductors

Let us suppose that we have two coils, and we know their inductances L_1 and L_2 and the coupling coefficient (k) between the two coils. If we know the mutual inductance (M) we can compute k from equation (1.3). The equivalent circuit representing the coupled inductors will be composed by a magnetising inductance L_m, which models the part of the coupled flux; a leakage inductance L_r models the flux losses, and an ideal transformer with an equivalent turn ratio n_{eq} (which is different from the turn ratio N_1/N_2, where N_1 and N_2 are the number of turns of primary and secondary coils). The equivalent circuit for coupled inductors is shown in figure 1.2. The following equations allow to compute the values of mutual inductance (1.4), leakage inductance (1.5) and equivalent turn ratio (1.6):

$$L_m = k^2 \cdot L_1 \tag{1.4}$$

$$L_r = (1 - k^2) \cdot L_1 \tag{1.5}$$

$$n_{eq} = k \cdot \sqrt{\frac{L_1}{L_2}} = k \cdot \frac{N_1}{N_2} \tag{1.6}$$

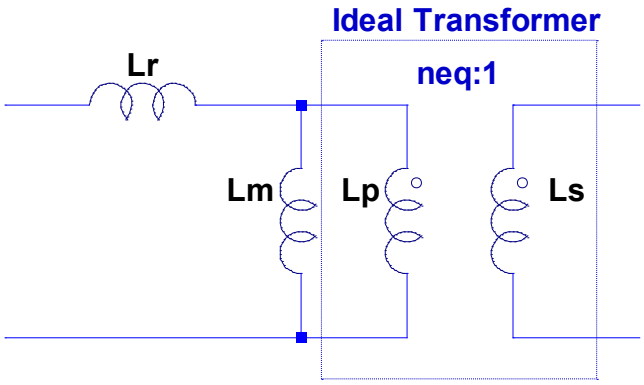

Figure 1. 2: equivalent circuit for coupled inductors

In the graph in figure 1.3, it is possible to see how the leakage inductance L_r and the mutual inductance L_m change as a function of k (equations (1.4) and (1.5)). In this graph, L_r and L_m are normalized respect to L1. Let us focus on three points of the graph:

- k = 1: magnetising inductance L_m is equal to L_1 and leakage inductance L_r is equal to zero
- k = 0: leakage inductance is equal to L_1 and mutual inductance L_m is equal to zero
- k = 0.7: this is the value of k for which L_r and L_m are equal

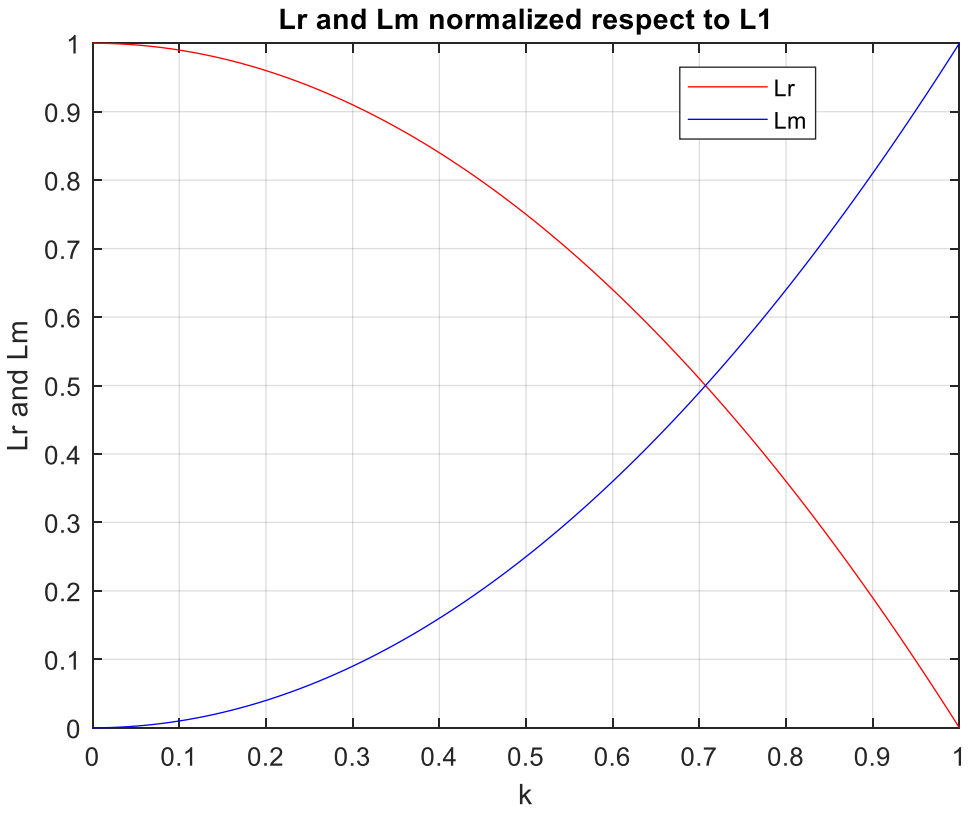

Figure 1. 3: Lr and Lm (normalized) as a function of k

2. Resonant Converters

2.1 Soft-Switching (ZVS and ZCS)

In high frequency converters the main problems and limits are due to the switching losses. These losses occur during the turn-on and turn-off of the switches (MOSFET, BJT). When the transistor is off, it doesn't absorb power because there is no current flowing through it. When the transistor is on, the power absorbed is almost zero, because the transistor is in triode region. Even though some current flows through the switch, the equivalent resistance (transconductance resistance) of transistor is low (about some milliohms). When the switching frequency of a MOSFET is high during turn-on and turn-off, there could be some instants in which the drain-source current and voltage overlap. Therefore, the absorbed power of the switches increases. This switching mode is called Hard-Switching.

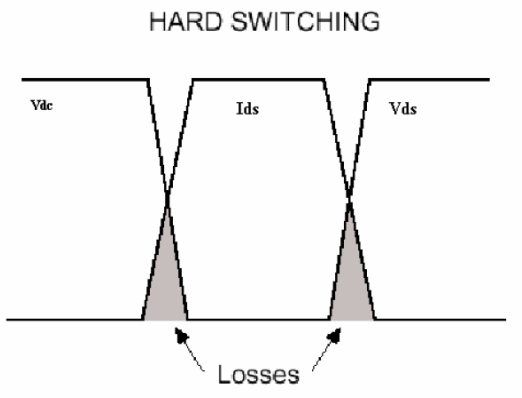

Figure 2. 1: Hard-Switching example

Resonant converters were created with the aim to resolve the problem due to the Hard-Switching; in fact, they are based on the so called Soft-Switching. In order to eliminate the area due to the overlap between current and voltage (which correspond with power absorbed by the switch, that is losses), the voltage has to reach zero volt before the current starts to flow through the switch, i.e., before the switch turns on. This is called Zero-Voltage-Switching (ZVS). Moreover, during the turn-off, the current through the switch must reach zero before the voltage on the switch increases: Zero-Current-Switching (ZCS). In figure 2.2 there are two examples of ZVS (only during switch's turn-on) and ZCS (only during switch's turn-off).

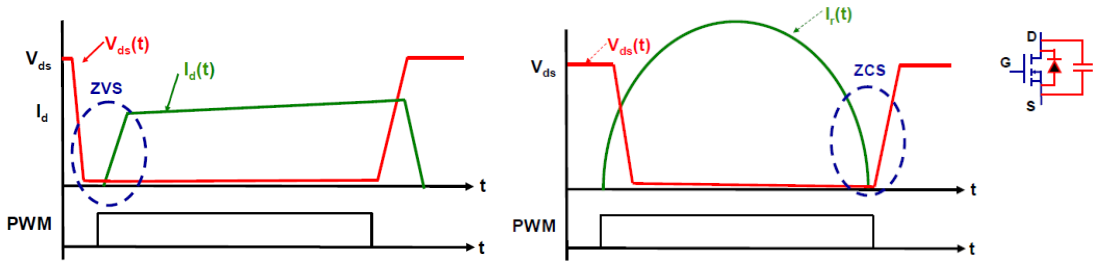

Figure 2. 2: Zero-Volt-Swithing and Zero-Current-Switching examples

PWM is the Pulse Width Modulator signal, that is the signal that drives the switches making them work alternatively in cut-off region and in triode region. Resonant converters are usually driven with frequency modulation. This means that the duty cycle is constant, while the frequency varies.

2.2 LLC Resonant Converter

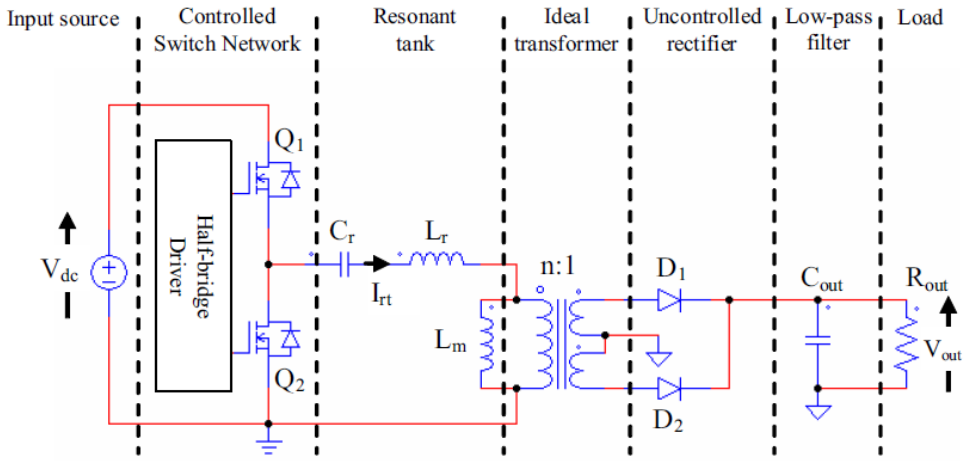

Figure 2. 3: LLC resonant converter's sections

In recent years, resonant converters have become very popular and were applied in various applications. In particular, the so-called LLC resonant converter seems to be one of the topologies with the most favourable benefit/drawback ratio. The reason is because LLC resonant converter can easily achieve high efficiency and can allow high frequency operations through soft switching. In figure 2.3 all the sections of an LLC resonant converter are shown.

In general, we can think the LLC converter as three macro blocks (figure 2.4):

- Square wave generator.
- Resonant network.
- Rectifier network.

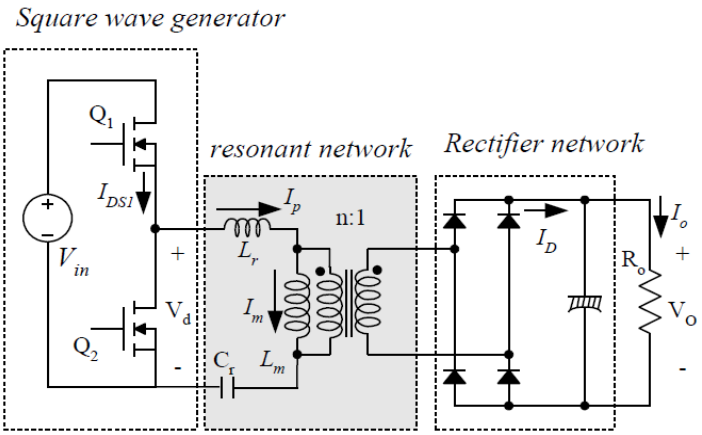

Figure 2. 4: the three macro blocks of LLC resonant converter

Square wave generator is composed by a controlled switching network which usually can be of two types: Half-Bridge or Full-Bridge. In this thesis it will be a Half-bridge type. It turns the V_{DC} input voltage into a square wave driving two switches (Q1 and Q2) alternately with a 50% duty cycle for each switch. The 50% duty cycle helps to balance the stress of switches. A small dead time is introduced between the transitions to prevent cross-conduction of the two switches and to ensure Zero-Volt-Switching (this concept will be explained in chapter 4). The square wave is applied at the input of the second block, the resonant network.

The resonant network is made of two parts: the resonant tank and an ideal transformer. The resonant tank consists of a resonant capacitor C_r and a resonant inductor L_r. It acts as a filter whose resonant frequency can be expressed as:

$$f_r = \frac{1}{2\pi\sqrt{(L_r \cdot C_r)}}$$

(2. 1)

Ideally, the harmonic waveforms of the input square wave are filtered by the resonant tank. This results in a sinusoidal load current flowing through resonant tank and through primary side of ideal transformer. We can see the resonant network like a voltage divider made of resonant tank and inductance L_m. L_m is the magnetizing inductance of the transformer, which (for an ideal transformer) has about the same value of the inductance of the primary winding. When the switching frequency is at the resonant frequency of resonant tank, the voltage on L_m is the same of the input voltage, because impedance of resonant tank is zero. The voltage on L_m decreases if switching frequency moves away from resonant frequency, because resonant tank impedance increases. The voltage divider ratio is frequency dependent. When circuit operates at resonant frequency, input current and output current are exactly in phase. As a consequence, both high side and low side switches are switching with zero current.

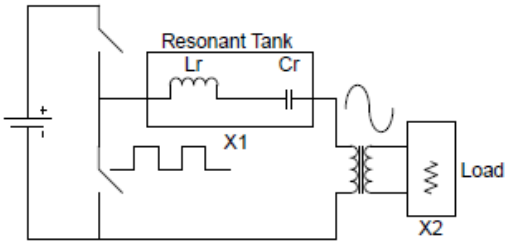

Figure 2. 5

The rectifier network produces DC voltage first rectifying the AC current with diode rectifier circuit, then with a capacitive output filter (low pass filter). The diode rectifier circuit can be made with a bridge rectifier or with a center-tapped rectifier. The first option is favourited when at the output there are low voltage and high current. The second is preferred when at the output there are high voltage and low current.

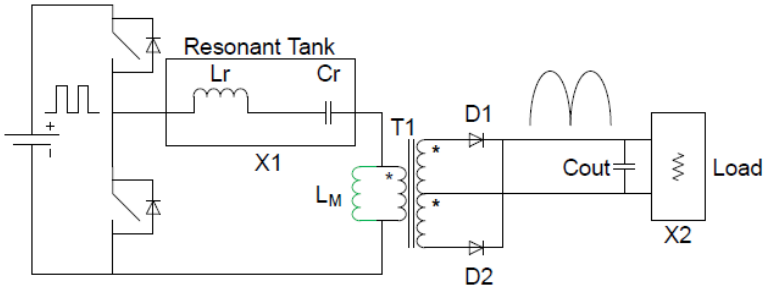

Figure 2. 6

2.3 First Harmonic Approximation (FHA)

We can express the square voltage at the input of the resonant tank in Fourier series:

$$V_{HB}(t) = \frac{V_{DC}}{2} + \frac{2}{\pi} \cdot V_{DC} \cdot \sum_{n=1,3,5} \frac{1}{n} \sin(n2\pi f_{sw} t)$$

(2. 2)

The fundamental component is:

$$V_{i,FHA}(t) = \frac{2}{\pi} \cdot V_{DC} \cdot \sin(2\pi f_{sw} t)$$

(2. 3)

With First Harmonic Approximation (FHA) we suppose that only purely sinusoidal current flows through resonant tank. Consequently, the resonant current will be:

$$I_{i,FHA}(t) = \sqrt{2} \cdot I_{RMS} \cdot \sin(n2\pi f_{sw} t - \varphi)$$

(2. 4)

Where I_{RMS} is the rms value of resonant current. φ is the phase shift of the resonant current respect to the fundamental component of input voltage. In fact, resonant current can lag or lead the fundamental voltage, and this depends on the impedance of the resonant tank. This happens when switching frequency moves away from resonant frequency. Depending on if the switching frequency is higher or lower than resonant frequency, the behaviour of the resonant tank can be dominated by inductive reactance or capacitive reactance. If the circuit works at resonance frequency, the phase shift will be zero. Through First Harmonic Approximation, the analysis of LLC circuit becomes simpler. In fact, if the LLC converter works around resonant frequency, only the fundamental frequency of input square wave can pass through the resonant tank. All the harmonics are filtered by resonant tank and only the fundamental component of square-wave voltage input contributes to the power transfer to the output. Now, let us consider the rectifier network and the output filter part. The primary-side circuit is replaced by a sinusoidal current source, I_{ac}, and a square wave voltage V_{RI}; the latter appears at the input of the rectifier.

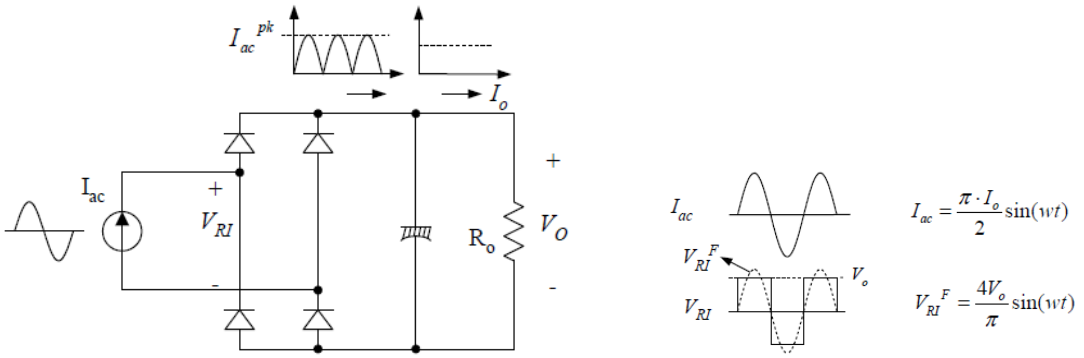

Figure 2. 7: secondary side waveforms

Since the average of $|I_{ac}|$ is the output current I_o, I_{ac} is obtained as:

$$I_{ac}(t) = \frac{\pi \cdot I_o}{2} \sin(2\pi f_{sw} t)$$

(2. 5)

The expression of the square wave voltage is:

$$V_{RI}(t) = \frac{4}{\pi} \cdot V_o \cdot \sum_{n=1,3,5} \frac{1}{n} \sin(n2\pi f_{sw} t)$$

(2. 6)

The fundamental component of V_{RI} is given as:

$$V_{RI}^{F} = \frac{4 \cdot V_o}{\pi} \sin(2\pi f_{sw} t)$$

(2. 7)

The rectifier circuit in the secondary side acts as an impedance transformer. Consequently, the equivalent load resistance is different from actual load resistance. Since harmonic components of V_{RI} are not involved in power transfer, the AC equivalent load resistance can be calculated by dividing V_{RI} by I_{ac} (which are in phase):

$$R_{ac} = \frac{V_{RI}^{F}}{I_{ac}} = \frac{8}{\pi^2} \cdot \frac{V_o}{I_o} = \frac{8}{\pi^2} \cdot R_o$$

(2. 8)

To obtain the equivalent load resistance shown in the primary side, we have to consider the transformer turn ratio:

$$n = \frac{N_p}{N_s}$$

(2. 9)

Where N_p is the number of turns of primary coils and N_s is the number of turns of secondary coils. As a consequence, the equivalent resistance seen from primary side is:

$$R_{ac} = \frac{8}{\pi^2} \cdot n^2 \cdot R_o$$

(2. 10)

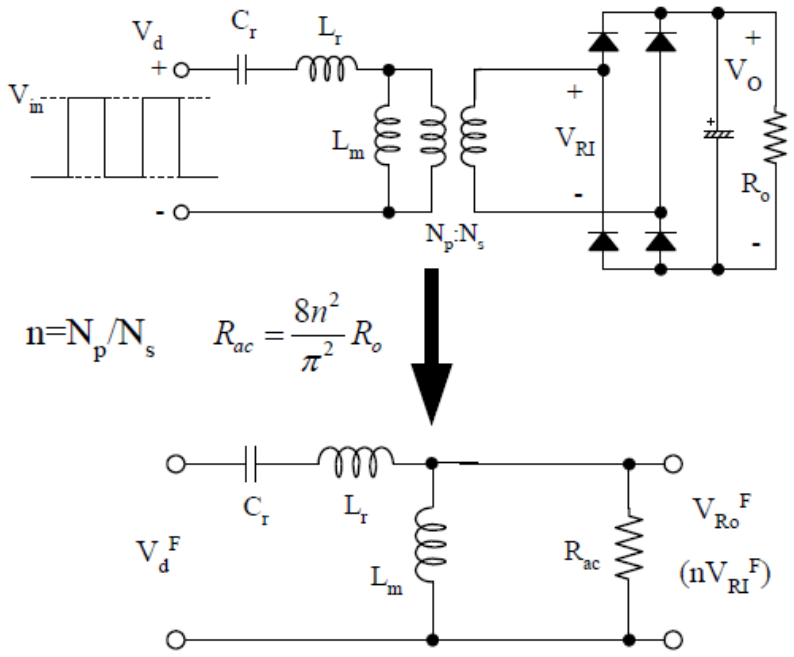

Figure 2. 8: FHA equivalent circuit at primary side

Now, with the equivalent AC circuit obtained, it can be demonstrated that the ratio between the output DC voltage V_{out} and the input DC voltage V_{in} is defined by the following expression:

$$\frac{V_{out}}{V_{in}} = \frac{1}{2n} \cdot M(f_{sw})$$

(2. 11)

Where M is called the voltage gain and can be expressed as:

$$M(f_n, \lambda, Q) = \frac{1}{\sqrt{\left(1 + \lambda - \frac{\lambda}{f_n^2}\right)^2 + Q^2\left(f_n - \frac{1}{f_n}\right)^2}}$$

(2. 12)

LLC resonant converter parameter definitions:

Resonant frequency: $f_{r1} = \frac{1}{2\pi\sqrt{(L_r.C_r)}}$

(2. 13)

Characteristic impedance: $Z_o = \sqrt{\frac{L_r}{C_r}}$

(2. 14)

Quality factor: $Q = \frac{Z_o}{R_{ac}}$

(2. 15)

Inductance ratio: $\lambda = \frac{L_r}{L_m}$

(2. 16)

Normalized frequency: $f_n = \frac{f_{sw}}{f_{r1}}$

(2. 17)

The LLC converter has also a second resonant frequency (f_{r2}) which depends on C_r, L_r and L_m. This resonance frequency refers to the no-load condition or when the secondary side diodes are not conducting, so also L_m resonates with L_r and C_r:

$$f_{r2} = \frac{1}{2\pi\sqrt{((L_r + L_m) \cdot C_r)}}$$

(2. 18)

We can see, from equation (2.19), that when the circuit is working at a frequency equal to the resonance frequency ($f_{sw} = f_{r1}$), the normalized frequency is unitary, and therefore the gain M is also unitary and independent from the load. So, the ratio between the output DC voltage V_{out} and the input DC voltage V_{in} becomes:

$$M = \frac{2 \cdot n \cdot V_{out}}{V_{in}} = 1$$

(2. 19)

This equation and equation (2.13) are the main equations to be considered for the design of an LLC resonant converter. In fact, if the converter works at resonance, the output voltage depends only on input voltage and turn ratio of transformer n:

$$V_{out} = \frac{V_{in}}{2 \cdot n}$$

(2. 20)

Under no-load condition, which means that R_{ac} tends to infinite and consequently Q is equal to zero, the voltage gain assumes the following form:

$$M(f_n, \lambda) = \frac{1}{\left|1 + \lambda - \frac{\lambda}{f_n^2}\right|}$$

(2. 21)

If normalized frequency goes to infinity, voltage gain tends to an asymptotic value:

$$M_\infty = M(f_n \to \infty, \lambda) = \frac{1}{1 + \lambda}$$

(2. 22)

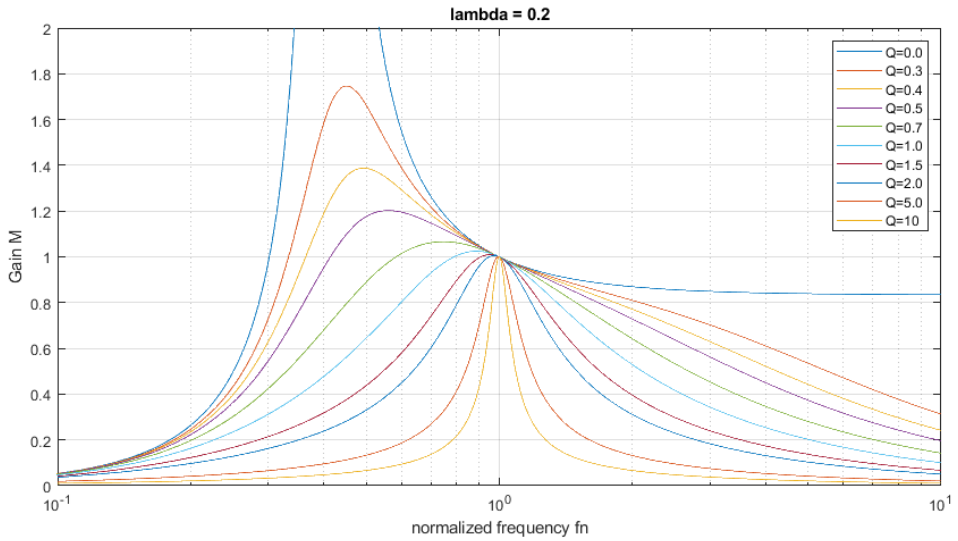

Figure 2. 9: LLC resonant converter's gain transfer function for different values of Q (λ =0.2)

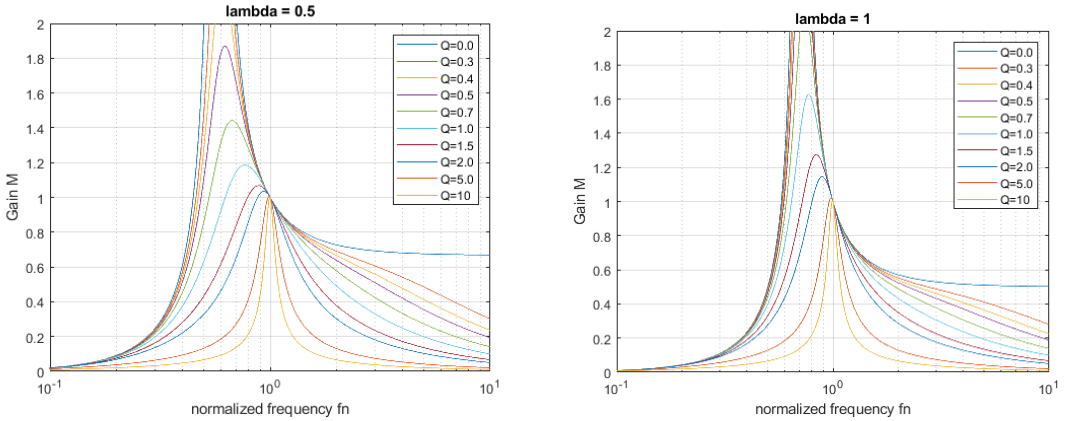

Figure 2. 10: : LLC resonant converter's gain transfer function (λ=0.5 and λ=1)

If lambda (the ratio between L_r and L_m, equation (2.15)) increases, the gain characteristic becomes narrower (figure 2.10). As a consequence, the gain is more sensitive to a frequency variation.

2.4 Operating Regions of LLC

The value of the switching frequency with respect to the resonance frequency, characterize the operation of the LLC resonant converter.

- $f_{sw} = f_{r1}$: the LLC converter works at resonance
- $f_{sw} < f_{r1}$: the LLC converter works below resonance
- $f_{sw} > f_{r1}$: the LLC converter works above resonance

ZVS can be achieved in specific conditions even in below and above resonance. As a function of the rectifier current, LLC can work in two operating modes: Continuos-Conduction-Mode (CCM) and Discontinuos-Conduction-Mode (DCM). If resonant current is high enough, the two rectifier diodes conduct current alternatively and LLC works in CCM. If resonant current is not high enough to turn on the diodes, the rectifier goes to DCM. The major factor that makes work LLC in CCM or DCM is the load current: at high load current, LLC works in CCM because D1 and D2 alternatively conduct current to the load. Whereas in presence of high load (low output current), LLC converter works in DCM because there are some intervals in which the rectifiers do not provide any current to the load. The characteristic of an LLC resonant converter can be divided into three regions (figure 2.11):

- Above resonance (ZVS)
- Below resonance (ZVS)
- Below resonance (ZCS)

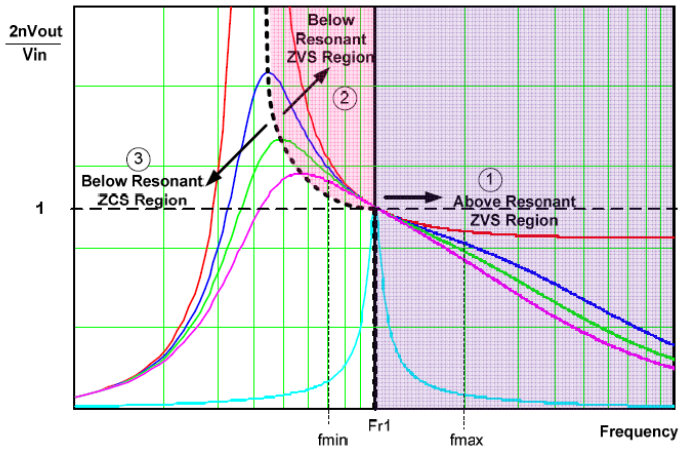

Figure 2. 11: the three working regions of LLC resonant converter

2.4.1 Above resonance (ZVS)

In region 1 (the purple shaded area) the switching frequency is higher than resonant frequency f_{r1}. In this region L_m never resonates with resonant capacitor C_r. L_m is clamped by the output voltage and acts as the load of the series resonant tank. This is the inductive load region, and the LLC converter is always under ZVS operation regardless of the load condition.

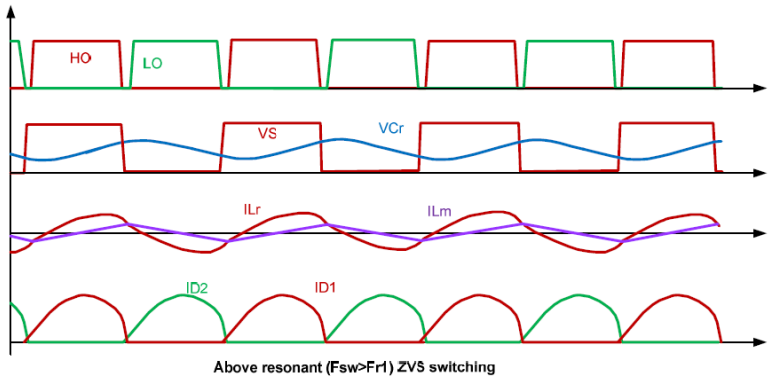

Figure 2. 12: Above resonance ($f_{sw} > f_{r1}$) ZVS switching

2.4.2 Below resonance (ZVS)

In region 2 the switching frequency is between the two resonant frequency f_{r1} and f_{r2}, it's the pink area in figure 2.11. The lower resonant frequency varies with load, so the boundary of region 1 and 2 traces the peak of the family load vs. gain curves. The ZVS

operation in this region is guaranteed by operating the converter to the right side of the load gain curve. If the switching frequency is below the resonant frequency f_{r1}, the LLC converter could work in either region 2 or region 3 depending on the load condition.

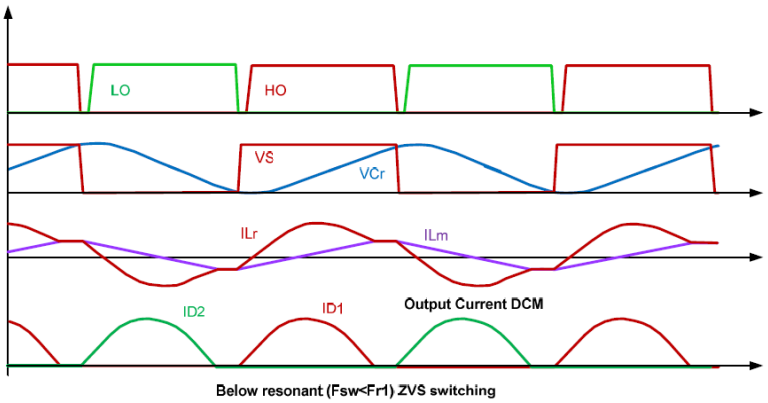

Figure 2. 13: Below resonance ($f_{sw} < f_{r1}$) ZVS switching

2.4.3 Below resonance (ZCS)

Region 3 is below resonance frequency and below the load curve. Here the LLC converter operates in capacitive mode and the two switches work under hard switching, so they have high switching losses. In this region there is Zero Current Switching (ZCS) and this region should always be avoided. In ZCS mode the two switching devices M1 and M2 are turned off under zero current condition. The turn-on of the two switches is in hard switching, so not under zero voltage switching (ZVS). Consequently, the switching losses during turn-on are high and the resonant capacitor Cr has high voltage stress.

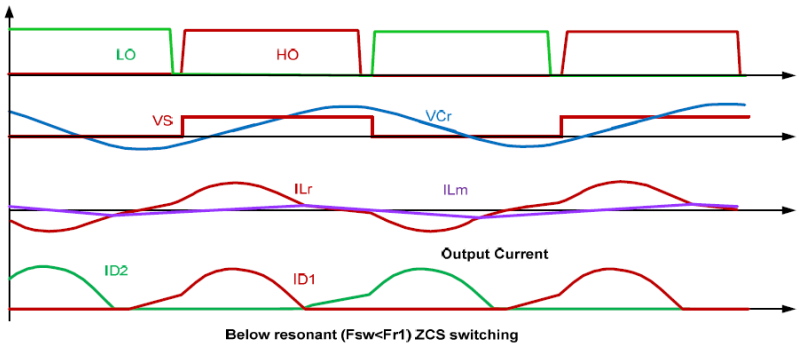

Figure 2. 14: Below resonance ($f_{sw} < f_{r1}$) ZCS switching

3. LLC for Wireless Power Transfer

Nowadays, as explained in chapter 1, Wireless Power Transfer (WPT) is getting popular thanks to its benefits. This kind of energy transfer mode has lots of practical applications. For example, it can be employed for smartphone charging pads, charging systems for medical sensor in human body or electric vehicle wireless charging systems. About this last point, electric vehicles are beginning to be a concrete reality which we can observe in our cities. In fact, in this period we can see a process of change and evolution about transportation technologies. Due to the necessity of pollution reduction, combustion-based vehicle will be substituted with less pollution vehicles. One example are the electric bicycle and scooters. They are generally used in the population for short trips and have limited power. Usually, the chargers are designed with direct contact with the vehicle through connectors whose contacts present a low resistance. This method simplifies the design but produces some problems which derive from the maintenance of the contacts, which degrade with the utilization. Furthermore, it's not helpful for user's comfort. On the contrary, wireless charger can provide comfort to the users, but there are some drawbacks related to this technology. In fact, the design becomes more complex, performance penalty could be present, and the high emission of electromagnetic radiations should be taken into account to respect the EMC standards. WPT techniques are often implemented in DC-DC converters. In fact, lots of wireless applications supplied by batteries are charged by DC power source.

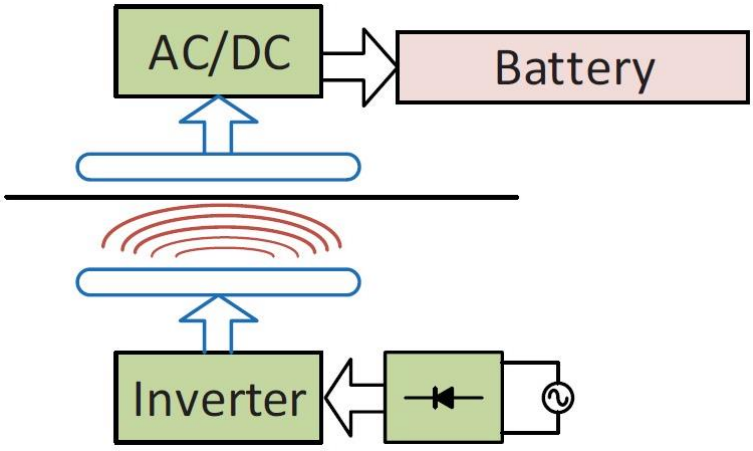

Figure 3. 1: basic wireless charger scheme

This charger must be designed properly in order to fulfil the specification of batteries. In the literature, lots of wireless power systems are implemented with LLC resonant converter. In fact, LLC resonant converter is a good choice to be implemented for WPT, due to its soft-switching characteristic and high efficiency at high frequency. The design of an LLC resonant converter for WPT it's a little different from designing a traditional

LLC. The main difference respect to the traditional LLC circuit is that the transformer is replaced with coils that are not well coupled.

Figure 3. 2: transformer

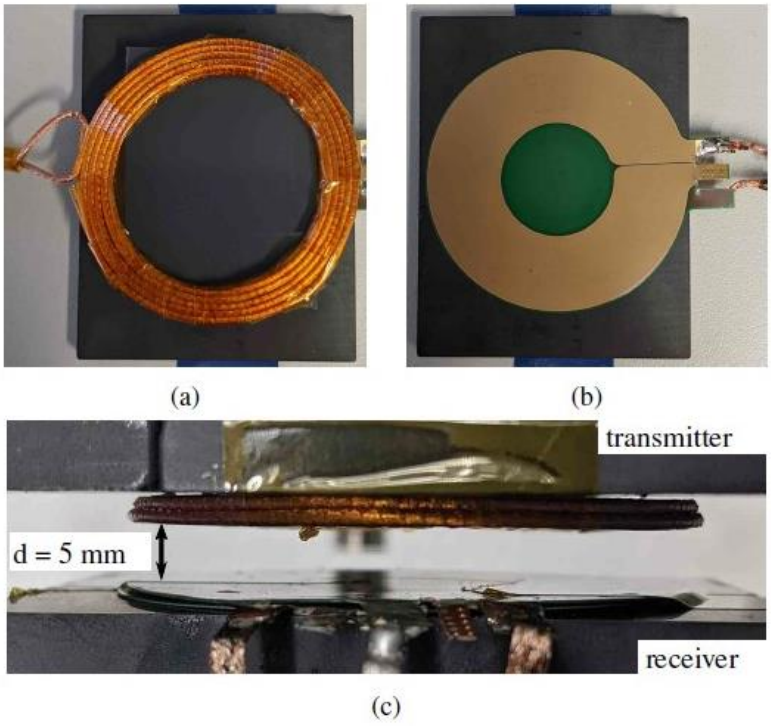

Figure 3. 3: (a) Transmitting coil, (b) receiving coil of center-tapped type, (c) side view

As explained in chapter 1, coupled inductors have low value of k and consequently a large leakage inductance, even larger than magnetizing inductance. This leakage inductance can be treated as the resonant inductance L_r of the LLC, so we don't need to add another inductor like in a classic LLC. This may be seen as an advantage deriving from using coupled inductors. But there are also disadvantages deriving from using coupled inductors in an LLC resonant converter: in an LLC with transformer (ideally with k = 1) L_m, L_r and turn ratio n are fixed. In fact, L_r is the inductance of a physical inductor that is placed in the circuit, L_m is the magnetising inductance of transformer and n is the turn ratio of the transformer. With coupled inductors L_r, L_m and n_{eq} all three depend on coupling coefficient k, which is sensitive to the distance between the two coils.

Furthermore, L_r varies the resonant frequency f_{r1} (2.13), which is one of the key parameters of LLC resonant converters. Equivalent turn ratio n_{eq} also varies a key parameter of LLC converter, that is the gain expression at resonance (2.19). In the literature, where the design of an LLC is proposed, the ratio between L_m and L_r is chosen between 2 and 10. This ratio defines the distance between the two resonance frequencies of LLC converter, and high values of it ensure a wide gain characteristic. Quality factor Q of LLC also depends on L_r and should be about 0.5. With coupled inductors, leakage inductance is higher than magnetizing inductance, especially for low values of k. Therefore, the ratio between L_m and L_r is lower than 1 (figure 2.10). Consequently, the gain characteristic becomes tighter since the two resonant frequencies are very close. The gain becomes very sensitive on the frequency since the curve is narrower. In this thesis the design of an LLC converter for WPT described in the paper [14] was taken in account. In this paper, the aim is to design a charger for the battery of electric bicycles. The design of the paper will be analysed and optimized in chapter 5.

4. Design with FHA

4.1 Input impedance and ZVS constraints

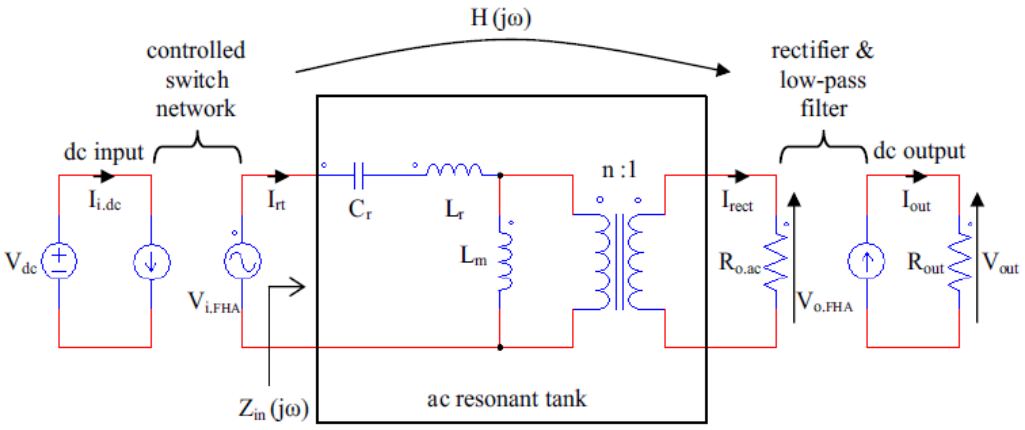

Figure 4. 1: LLC resonant converter two-port model

In figure 4.1 there is the two-port model of the LLC resonant converter under FHA. The AC resonant tank model can be defined by its forward transfer function H(s) and input impedance $Z_{in}(s)$.

$$H(s) = \frac{V_{oFHA}(s)}{V_{iFHA}(s)} = \frac{1}{n}\frac{n^2 R_{oac}||sL_m}{Z_{in}(s)} \tag{4.1}$$

$$Z_{in}(s) = \frac{V_{iFHA}(s)}{I_{rt}(s)} = \frac{1}{sCr} + sL_r + n^2 R_{oac}||sL_m \tag{4.2}$$

From equation (4.2) the normalized input impedance of resonant tank can be computed:

$$Z_n(f_n, \lambda, Q) = \frac{Z_{in}(f_n, \lambda, Q)}{Z_o} = \frac{jf_n}{\lambda + jf_n Q} + \frac{1 - f_n^2}{jf_n} \tag{4.3}$$

In figure 4.2 the magnitude of the normalized input impedance is represented. The blue and red curves in this figure represent the short-circuit and no-load cases respectively. All the curves, which differ by Q, converge at normalized crossing frequency $f_{n.cross}$. This is defined as:

$$f_{n.cross} = \sqrt{\frac{2\lambda}{1+2\lambda}} \tag{4.4}$$

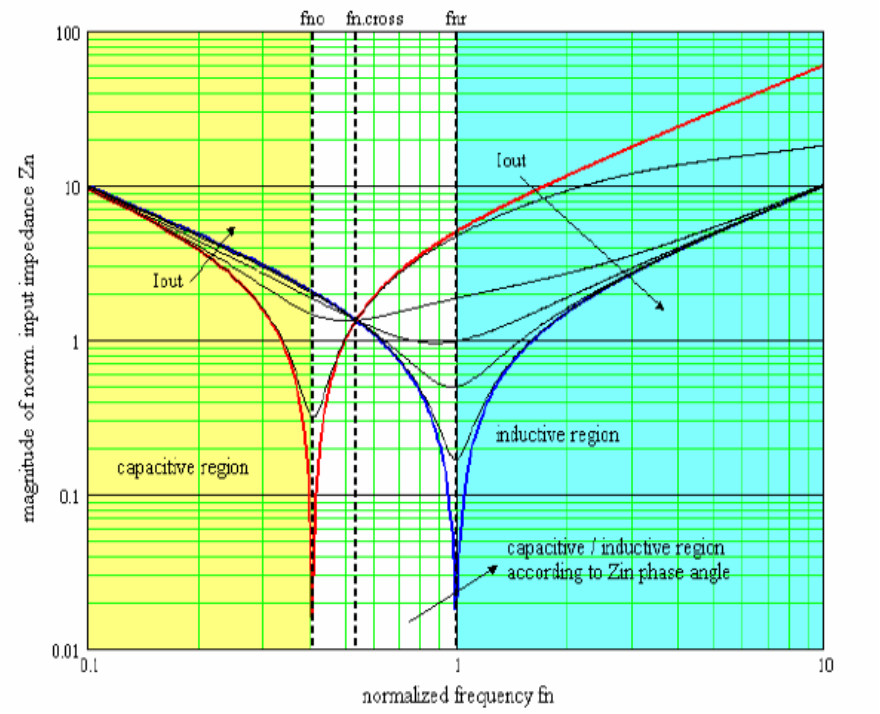

Figure 4. 2: Normalized input impedance

For a normalized frequency lower than f_{no} the input impedance is capacitive (capacitive region), and the tank current leads the half-bridge square voltage. For a normalized frequency higher than the resonance frequency (f_{nr}=1), right-hand side region, the input impedance is inductive (inductive region), and the resonant tank current lags the input voltage. In the region between the two resonance frequencies the input impedance can be either capacitive or inductive. This depends on the value of the impedance phase angle. In order to find the boundary condition between capacitive and inductive mode operation of the LLC resonant converter, we have to impose that the imaginary part of $Z_n(f_n,\lambda,Q)$ is zero, i.e., imposing that Z_{in} has zero phase angle. For a fixed couple (λ-Q), we can explicit the normalized frequency which ensure that the input resonant impedance is real (only real power is absorbed from the source):

$$f_{nZ}(\lambda, Q) = \sqrt{\frac{Q^2 - \lambda(1+\lambda) + \sqrt{[Q^2 - \lambda(1+\lambda)]^2 + 4Q^2\lambda^2}}{2Q^2}} \tag{4.5}$$

For a fixed normalized frequency and inductance ratio (f_n and λ) we can explicit the maximum value of quality factor ensuring that the tank impedance is inductive:

$$Q_Z(f_n,\lambda) = \sqrt{\frac{\lambda}{1-f_n^2} - \left(\frac{\lambda}{f_n}\right)^2}$$

(4.6)

The borderline between capacitive and inductive mode (in the region between the two resonance frequencies) is:

$$M_Z(f_n,\lambda) = \frac{f_n}{\sqrt{f_n^2(1+\lambda)-\lambda}}$$

(4.7)

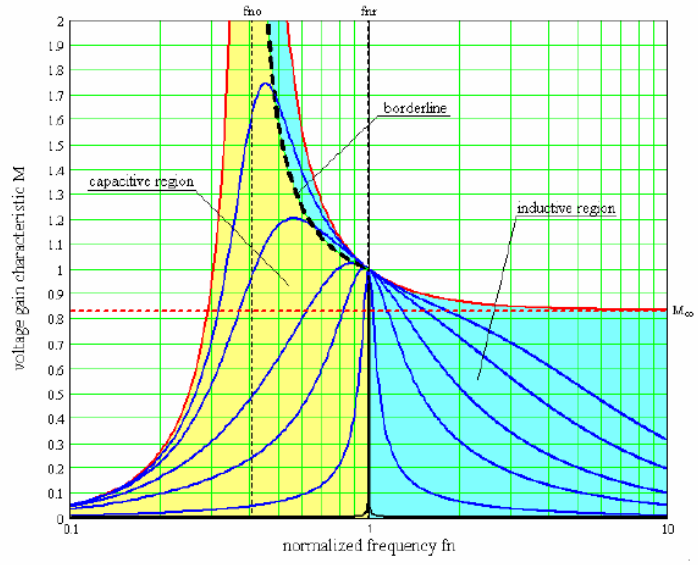

Figure 4. 3: capacitive and inductive region in M-fn plane

From equation (4.7) we can get the minimum operating frequency in order to obtain the required maximum voltage gain at the boundary between capacitive and inductive mode:

$$f_{n.min} = \sqrt{\frac{1}{1+\frac{1}{\lambda}\left(1-\frac{1}{M_{max}^2}\right)}}$$

(4.8)

Substituting equation (4.8) in equation (4.6), we obtain the maximum quality factor which allows the required maximum voltage gain at the boundary between capacitive and inductive mode:

$$Q_{max} = \frac{\lambda}{M_{max}} \sqrt{\frac{1}{\lambda} + \frac{M_{max}^2}{M_{max}^2 - 1}}$$

(4.9)

By equating the second term of (2.21) to the minimum voltage gain, it is possible to compute the expression of the maximum normalized frequency:

$$f_{n.max} = \sqrt{\frac{1}{1 + \frac{1}{\lambda}\left(1 - \frac{1}{M_{min}}\right)}}$$

(4.10)

The assumption that the LLC works in induction region it's a necessary but not sufficient condition to work in ZVS. This is because in FHA we neglect the parasitic capacitance of the half-bridge middle point, which needs energy to be charged and depleted during transition. Referring to the figure 4.4, the capacitor C_{OSS} is the effective drain-source capacitance of the power MOSFETs, while C_{stray} is the total stray capacitance present across the resonant tank impedance. So, the total capacitance C_{ZVS} at node N is:

$$C_{ZVS} = 2C_{OSS} + C_{stray}$$

(4.11)

We already told that a dead time T_D is inserted between the turn-off and the turn-on of the switches in order to ensure ZVS. So, during dead time T_D, both switches are not conducting and the voltage on node N during transition is $\Delta V = V_{DC}$. C_{ZVS} is depleted from inductor current I_{rt} which is still flowing in the circuit at the end of the first cycle due to the phase lag of the input current with respect to the input voltage. In this way, voltage goes from ΔV to zero. In order to guarantee ZVS, the tank current at the end of the first half cycle, must exceed the minimum value necessary to deplete C_{ZVS} during the dead time interval T_D, that is:

$$I_{ZVS} = C_{ZVS} \frac{\Delta V}{T_D}$$

(4.12)

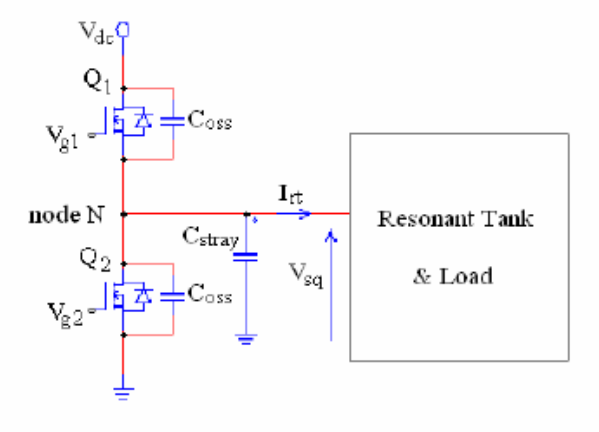

Figure 4. 4: parasitic capacitance

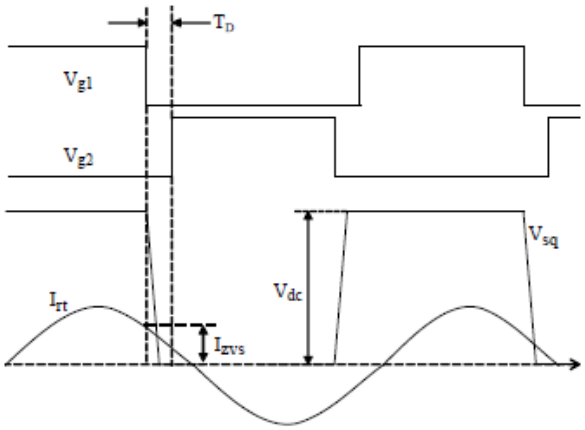

Figure 4. 5: Circuit behaviour at ZVS transition

$$\tan(\varphi) = \frac{Im[Z_n(f_n, \lambda, Q)]}{Re[Z_n(f_n, \lambda, Q]} \geq \frac{C_{ZVS} V_{dc}^2}{\pi T_D P_{in}}$$

(4 . 13)

Equation (4.13) is the sufficient condition to have ZVS for the half bridge power MOSFETs, but this solution is not convenient for the quality factor Q_{ZVS} that ensure ZVS behaviour at full load and minimum input voltage. We can compute the Q_{max} value (at maximum output power and minimum input voltage) where the input impedance has zero phase, and take some margin (5% - 10%):

$$Q_{ZVS.1} = 90\% \div 95\% \cdot Q_{max}$$

(4 . 14)

Then we have to check that the condition, expression (4.13), is satisfied at the end of the process, so the resonant tank has been completely defined. If the condition is not satisfied, the process can be iterated. The sufficient condition to work with ZVS must be also satisfied at no-load and maximum input voltage; in this case, we can find an

additional constrain on the maximum quality factor at full load to guarantee ZVS. The input impedance at no-load is the following:

$$Z_{in.OL}(f_n) = jZ_o\left[f_n\left(1+\frac{1}{\lambda}\right)-\frac{1}{f_n}\right]$$

(4.15)

The sufficient condition for ZVS in this operating condition is:

$$\frac{V_{i.FHAmax}}{|Z_{inOL}(f_{n.max})|} \geq \frac{I_{ZVS(Vdcmax)}}{\sqrt{2}}$$

(4.16)

The constrain of the quality factor for ZVS at no-load and maximum input voltage is:

$$Q_{ZVS2} \leq \left(\frac{2}{\pi}\right)\left(\frac{\lambda f_{nmax}}{(\lambda-1)f_{nmax}^2-\lambda}\right)\left(\frac{T_D}{R_{ac}C_{ZVS}}\right)$$

(4.17)

In order to guarantee ZVS over the whole operating range of the resonant converter, we have to choose a maximum quality factor value lower than the smaller between $Q_{ZVS.1}$ and $Q_{ZVS.2}$.

4.2 Design procedure

In this section an LLC design procedure proposed from STMicroelectronics [15] will be explained.

Design specification:

- Input voltage range: $V_{dc.min}$ – $V_{dc.max}$
- Nominal input voltage: $V_{dc.nom}$
- Regulated output voltage: V_{out}
- Maximum output power: P_{out}
- Resonant frequency: f_r
- Maximum operating frequency: f_{max}

Additional info:

- Parasitic capacitance at node N: C_{zvs}
- Dead time of driving circuit: T_D

General criteria for the design

- The converter will be designed to work at resonance at nominal input voltage
- The converter must be able to regulate down to zero load at maximum input voltage
- The converter will always work in ZVS in the whole operating range

The procedure consists in 10 steps.

1. The gain M at nominal input voltage must be 1, so we can derive the turn ratio n:

$$M_{nom} = \frac{2 \cdot n \cdot V_{out}}{V_{dc.nom}} = 1 \rightarrow \ n = \frac{V_{dc.nom}}{2 \cdot V_{out}}$$

(4 . 18)

2. Compute the maximum and the minimum gains related to the boundary of input voltage:

$$M_{max} = \frac{2 \cdot n \cdot V_{out}}{V_{dc.min}}$$

(4 . 19)

$$M_{min} = \frac{2 \cdot n \cdot V_{out}}{V_{dc.max}}$$

(4 . 20)

3. Compute the maximum normalized frequency:

$$f_{n.max} = \frac{f_{max}}{f_r}$$

(4 . 21)

4. Compute the effective load resistance reflected at the primary of the transformer:

$$R_{ac} = \frac{8}{\pi^2} \cdot \frac{V_{out}^2}{P_{out}}$$

(4 . 22)

5. Now we must impose that the LLC converter works with zero load and maximum input voltage, at maximum frequency. From equation (4.10) we obtain:

$$\lambda = \frac{1 - M_{min}}{M_{min}} \cdot \frac{f_{max}^2}{f_{max}^2 - 1}$$

(4 . 23)

6. Compute the maximum Q value to operates in the ZVS region at minimum input voltage and full load condition (equation (4.9) and equation (4.14)):

$$Q_{ZVS.1} = 95\% \cdot Q_{max} = 95\% \cdot \frac{\lambda}{M_{max}} \sqrt{\frac{1}{\lambda} + \frac{M_{max}^2}{M_{max}^2 - 1}}$$

(4 . 24)

7. Compute the max Q value to work in the ZVS operating region at maximum input voltage and no-load condition (equation (4.17)):

$$Q_{ZVS2} = \left(\frac{2}{\pi}\right)\left(\frac{\lambda f_{nmax}}{(\lambda - 1) f_{nmax}^2 - \lambda}\right)\left(\frac{T_D}{R_{ac} C_{ZVS}}\right)$$

(4 . 25)

8. Chose the max quality factor for ZVS in the whole operating range:

$$Q_{ZVS2} \leq \min\{Q_{ZVS1}, Q_{ZVS2}\}$$

(4 . 26)

9. Compute the minimum operating frequency at full load and minimum input voltage, according to the following approximated formula:

$$f_{min} = f_r \sqrt{\frac{1}{1 + \frac{1}{\lambda}\left(1 - \frac{1}{M_{max}^{1+\left(\frac{Q_{ZVS}}{Q_{max}}\right)^4}}\right)}}$$

(4 . 27)

10. Compute characteristic impedance, resonance capacitance, resonance inductance and magnetizing inductance:

$$Z_o = Q_{ZVS} \cdot R_{ac}, \qquad C_r = \frac{1}{2\pi f_r Z_o}, \qquad L_r = \frac{Z_o}{2\pi f_r}, \qquad L_r = \frac{L_r}{\lambda}$$

(4 . 28)

4.3 Design example

In this section a design example is shown, according with the procedure just presented. The aim is to design an LLC resonant converter with the following specifics:

- Nominal input DC voltage: 390 V
- Input DC voltage range: from 320V to 420V
- Output voltages: 200V at 1.6A continuous current; 75V at 1A continuous current
- Resonance frequency: 120kHz
- Max operating frequency: 150kHz
- Delay time: 270ns
- Foreseen half-bridge total stray capacitance (at node N): 350pF

In the next table there are the results of various steps to design an LLC converter described in paragraph 4.3. The algorithm was implemented on MATLAB script which is exhibited in Appendix M.1.

Step	Parameters
1	N = 0.975
2	M_{max} = 1.2188, M_{min} = 0.9286
3	$f_{n.max}$ = 1.25
4	R_{ac} = 77.0548*
5	λ = 0.2137
6	$Q_{ZVS.1}$ = 0.4097
7	$Q_{ZVS.2}$ = 1.0117
8	Q_{ZVS} = 0.4097
9	f_{min} = 80.901 kHz
10	Z_o = 31Ω, C_r = 42nF L_r = 41μH, L_m = 195μH

*To compute R_{ac} we consider as R_{load} the average of load resistance considering the two output voltage and current cases:

$$R_{load} = \frac{\left(\frac{200V}{1.6A} + \frac{75V}{1A}\right)}{2} = 100\Omega \qquad (4.29)$$

From (2.10) we obtain R_{ac} = 77.0548Ω.

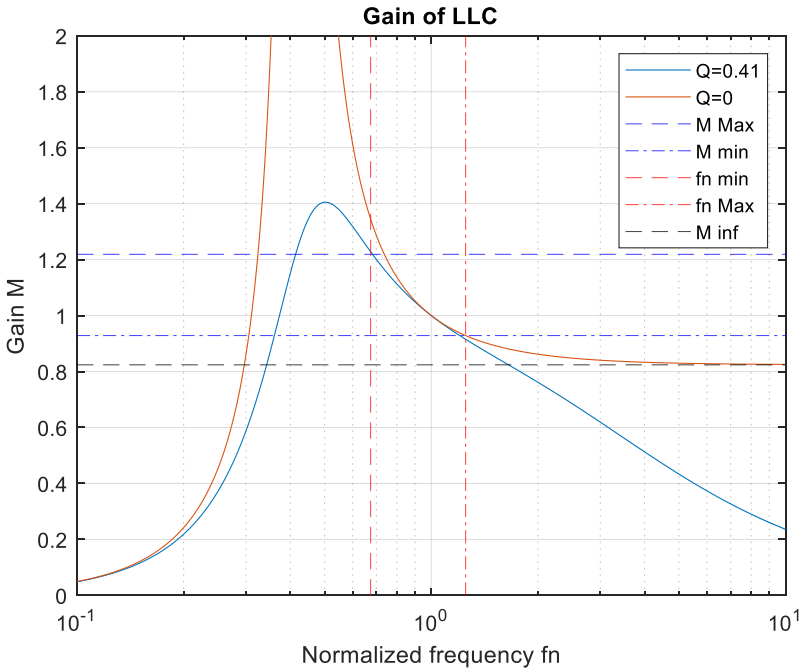

Figure 4. 6: LLC gain and frequency's borderline for ZVS

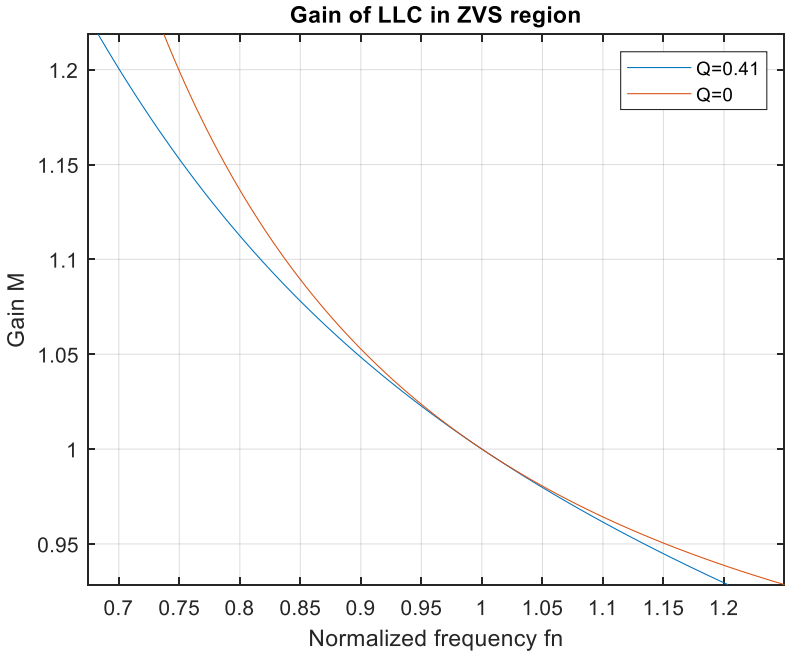

Figure 4. 7: LLC region to ensure ZVS

In figure 4.6 there is the plot of the gain at no load (red curve) and the gain for the max quality factor to ensure ZVS (blue curve). The dashed lines mark the boundaries of gain and normalized frequency to stay in ZVS. In figure 4.7 there is the plot of only ZVS region. In order to work in ZVS, the LLC resonant converter must stay between the red and blue curves. The gain value (2.12), i.e., the working point, depends as well as by normalized frequency, on quality factor Q (2.15) and inductance ratio λ (2.16). This design procedure

is useful to understand the behaviour of LLC resonant converter, but it does not take into account any source of losses and the non-idealities of the circuital elements. The latters are taken into account in the next design method, which focalizes only on the resonance working point, that is when switching frequency is equal to resonance frequency.

5. Design with steady-state switching sequence

5.1 Design at resonance with losses

First Harmonic Approximation (FHA) is a strongly simplified method for the design of an LLC resonant converter. In fact, it is not capable to consider any sources of loss due to non-idealities of the circuital elements. Consequently, FHA is not useful to define an accurate description of the LLC circuit. In other words, it cannot be accepted in practice. In order to obtain a realer model, a more analytic approach should be followed, i.e., searching for the solution of the LLC converter in the time-domain. A good method is the switching sequence approach. This method consists in dividing the switching period of the converter, at steady-state, into a succession of intervals (switching-states). In these intervals the circuit is described by the state of the semiconductor devices, which can be on or off. The behaviour of the circuits during the various intervals can be analytically solved in order to obtain an accurate expression of all the signals.

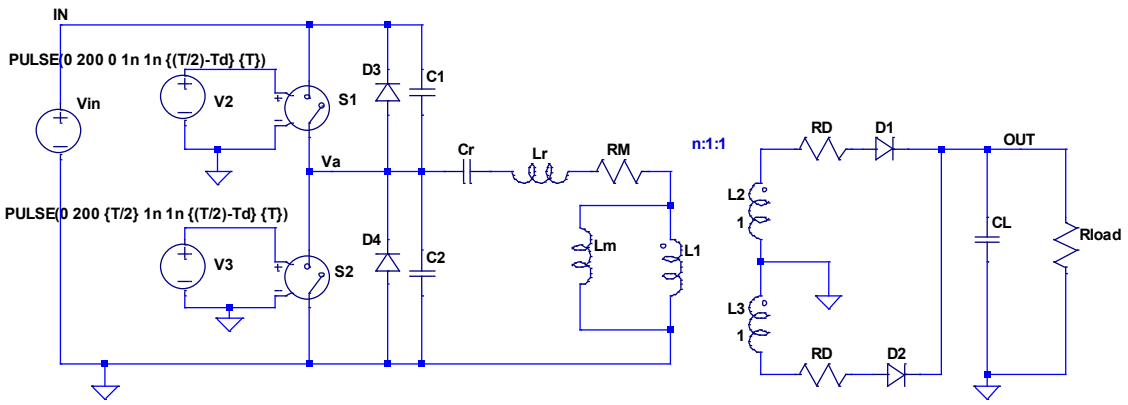

Figure 5. 1: LLC schematic on LTspice

In figure 5.1 there is the LTspice schematic of the circuit under analysis. The switching network is Half-Bridge type, where the MOSFETs are substituted with two switch models. The rectifier side is center-tapped type. For this analytical analysis we neglect the dead time and suppose that the LLC converter is working at resonance, since it is the preferred operating mode in which the LLC works. At resonance, the turn-on and turn-off of the MOSFETs are synchronized with turn-on and turn-off of the power diodes. Furthermore, the circuit is working at steady state. Under these assumptions, during every switching period the circuit works alternatively in two operating regions which alternate each other and each lasts half of the period. These operating regions are:

- **M1D1**: the high-side MOSFET M1 is on (short circuit) and low-side MOSFET M2 is off (open circuit). At node Va there is the input voltage V_{in}. Diode D1 is on while diode D2 is off
- **M2D2**: the low-side MOSFET M2 is on (short circuit) and high-side MOSFET M1 is off (open circuit). Node Va is grounded. Diode D2 is on while diode D1 is off

Neglecting the dead time, we can simplify the lossy circuit in this way:

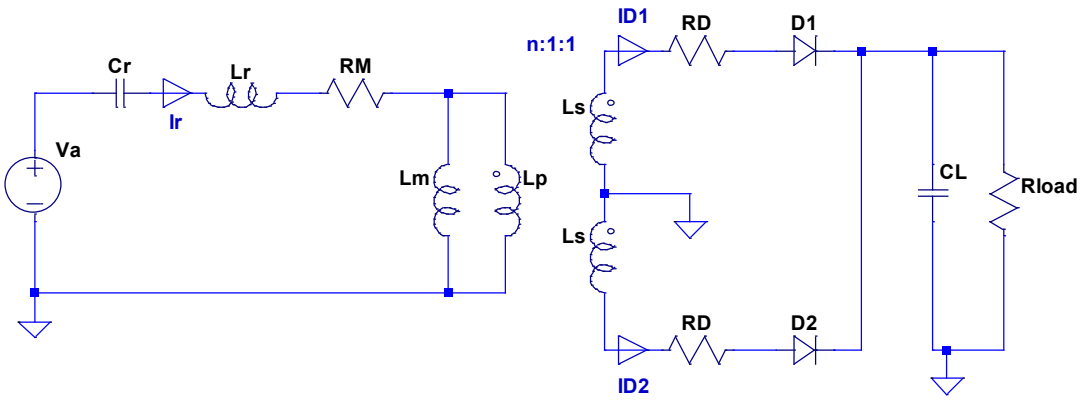

Figure 5. 2: LLC converter's switching sequence model

Referring to the circuit in figure 5.2, the voltage generator Va models the input voltage and the two MOSFETs (i.e., the square waveform at the input of resonant tank): when high-side MOSFET is on and low-side MOSFET is off, Va = Vin. When low-side MOSFET is on and high-side MOSFET is off, Va = 0V. The losses of circuital elements are also taken into account. Resistance RM models the losses of the MOSFETs (on-resistance of power transistors), equivalent series resistance (ESR) of resonance capacitance C_r and of inductance L_r. RD resistances model the losses of secondary inductance and forward resistance of diodes. If the circuit works at steady state, the regions M1D1 and M2D2 will alternate each other. In the next table, the characteristics of the two alternating regions are highlighted:

	M1D1	M2D2
Va	Vin	0V
M1	ON	OFF
M2	OFF	ON
D1	ON	OFF
D2	OFF	ON

5.2 MATLAB implementation

As just explained, if the LLC circuit works at resonance and if the dead time is neglected, at steady-state there will be two regions which alternate each other (M1D1-M2D2). For every operating region (i.e., for every equivalent circuit) a system of ODEs (Ordinary-Differential-Equations) can be defined. To resolve the system, the first step consists of choosing the state variables: resonant current I_r, resonant capacitor voltage V_{Cr} and secondary side current (I_{D1} or I_{D2}). The choice of these three state variables derives from the necessity to have a more practical design. In fact, from the current on the diodes I_{D1} and I_{D2}, the output DC current flowing through the load can be easily computed. The output current is related to the output power, which can be a project specification. The two half-period are described by a system of three ODEs. In this design, the forward voltage of diodes is also considered.

This is the system for the state M1D1:

$$\begin{cases} I_r = C_r \dfrac{dV_{Cr}}{dt} \\ V_{in} = R_M I_r + V_r + L_r \dfrac{dI_r}{dt} + L_m \dfrac{d\left(I_r - \frac{I_{D1}}{n}\right)}{dt} \\ V_{out} = \dfrac{L_m}{n} \dfrac{d\left(I_r - \frac{I_{D1}}{n}\right)}{dt} - R_D I_{D1} - V_{D1,on} \end{cases}$$

While the system for the state M2D2 is:

$$\begin{cases} I_r = C_r \dfrac{dV_{Cr}}{dt} \\ 0 = R_M I_r + V_r + L_r \dfrac{dI_r}{dt} + L_m \dfrac{d\left(I_r - \frac{I_{D2}}{n}\right)}{dt} \\ V_{out} = \dfrac{L_m}{n} \dfrac{d\left(I_r - \frac{I_{D2}}{n}\right)}{dt} - R_D I_{D2} - V_{D2,on} \end{cases}$$

To resolve the two systems, the *ode45* function of MATLAB was exploited. The systems were written on MATLAB in the matrix form $\underline{\mathbf{y}} = A \cdot \underline{\mathbf{x}} + b$, where $\underline{\mathbf{y}}$ is the vector of the derivatives of the state variables, while $\underline{\mathbf{x}}$ represents the vector of the state variables. Remember that if the circuit is at steady state, these two regions will alternate each other. The state M1D1 will begin to evolve with some initial conditions. The final conditions at the end of state M1D1 will be the initial conditions of state M2D2. As a

consequence, the final conditions of state M2D2 will be the initial conditions of state M1D1 and so on. The initial conditions of the systems are:

- V_{Cr_0}: Initial voltage on resonance capacitor C_r
- I_{D1_0}: Initial current on diode D1 (it must be 0)
- I_{Lr_0}: Initial resonant current to ensure ZVS

In order to determine the exact design, a MATLAB optimizer was exploited to find the optimal values of the circuit parameters. In particular, the optimizer evaluates the norm of the difference between two vectors of four elements. One vector contains the final values of the state variables (V_{Cr}, I_D, I_r) at the end of the state M2D2 (i.e., at the end of the switching period) and the output DC current (it is computed from the average of diodes current):

$$[V_{Cr}, I_{D2}, I_r, I_{out}]$$

The other vector contains the initial conditions of the three state variables (V_{Cr0}, I_{D1_0}, I_{Lr_0}) and the output DC current defined as $Vout/R_{load}$:

$$\left[V_{Cr\_0}, I_{D1\_0}, I_{r\_0}, V_{out}/R_{Load}\right]$$

The optimizer tries to minimize the norm of the difference between the two vectors by varying four parameters: initial voltage on resonant capacitor V_{Cr_0}, turn ratio of transformer n, magnetising inductance L_m and switching period T.

$$\left[V_{Cr\_0}, n, L_m, T\right]$$

Trying to minimize the norm of the difference between these two vectors means that the final values of state M2D2 should match with the initial values of the switching states (initial value of M1D1). The MATLAB optimizer reiterates the process until the norm is lower than a certain threshold ($1x10^{-9}$). This means that the optimization process is over. The MATLAB script is presented in Appendix M.2.

5. Design with steady-state switching sequence

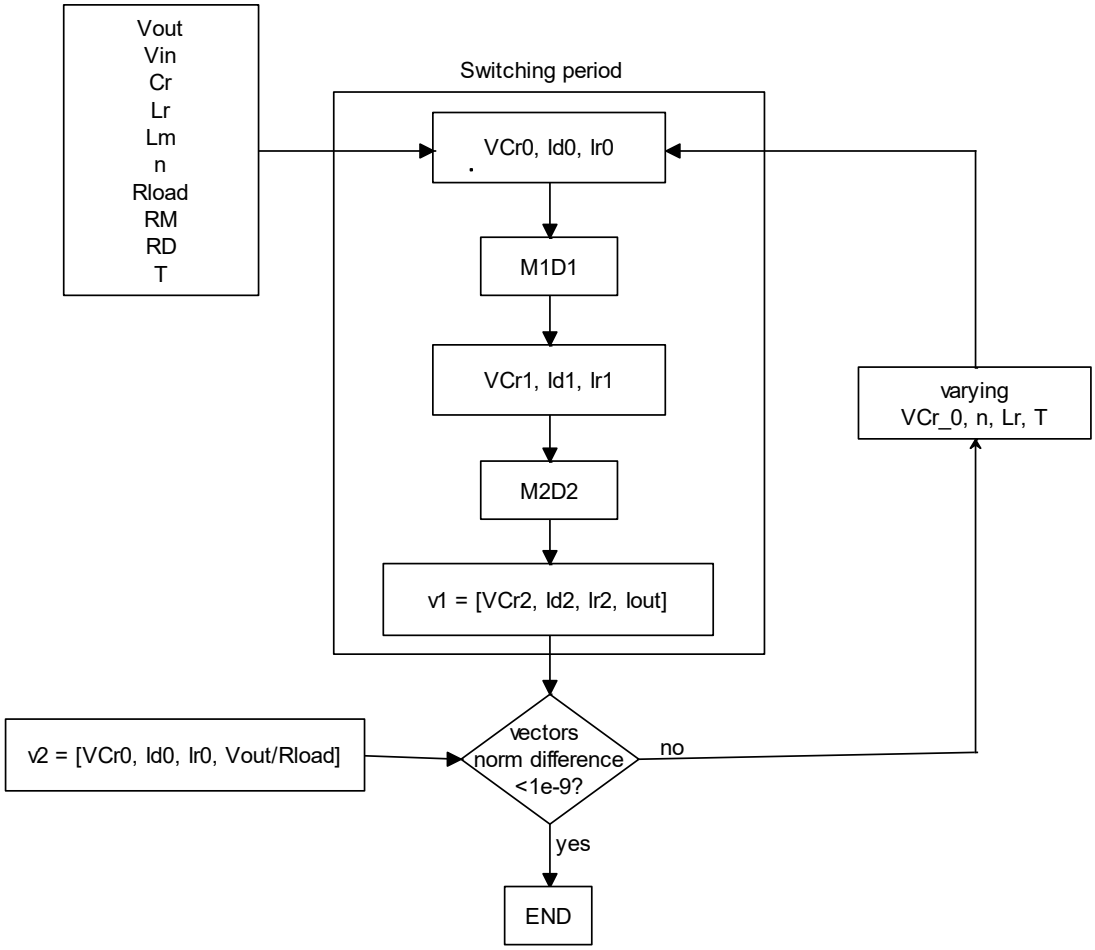

Figure 5. 3: algorithm flow chart

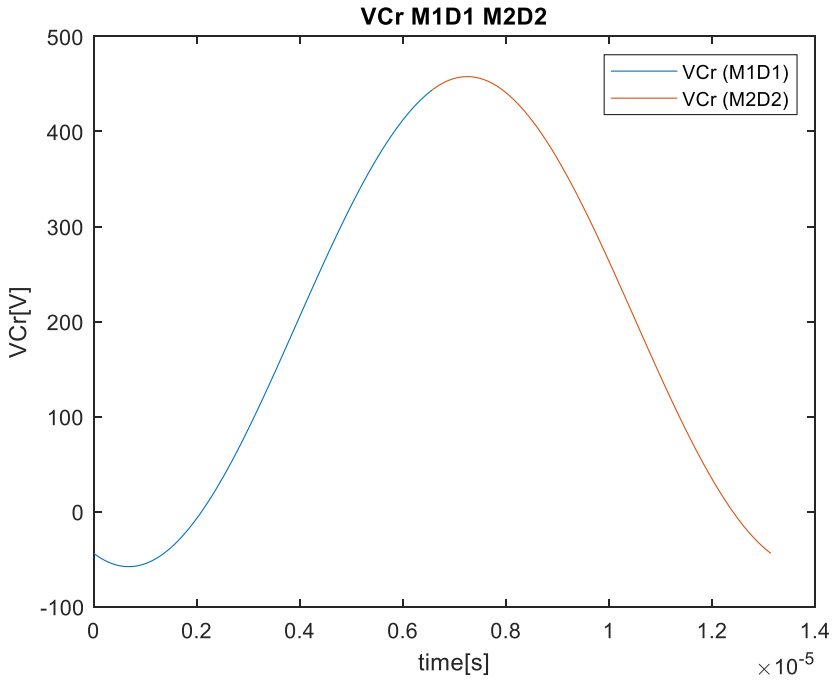

Figure 5. 4: voltage across Cr during M1D1 (blue) and M2D2 (red)

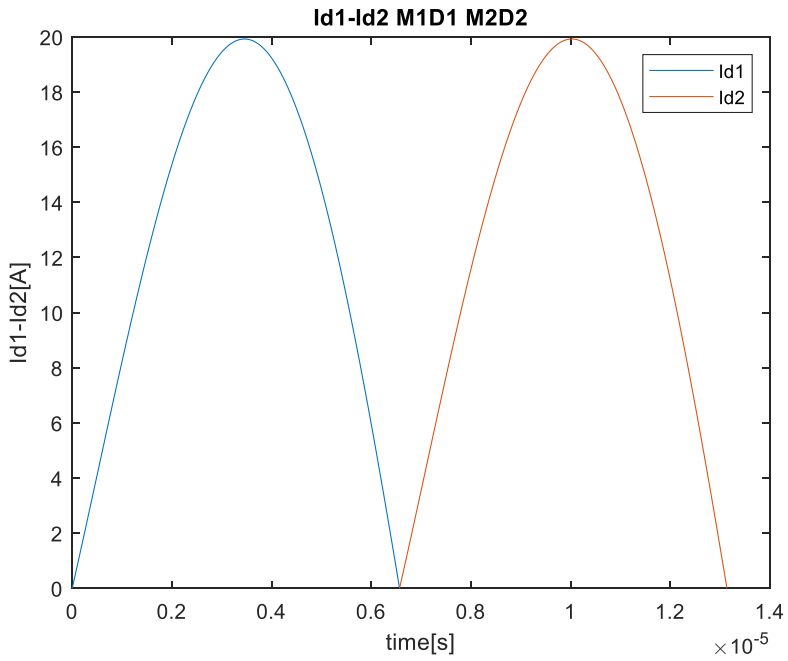

Figure 5. 5: current on D1(blue) and D2 (red) during M1D1 (blue) and M2D2 (red)

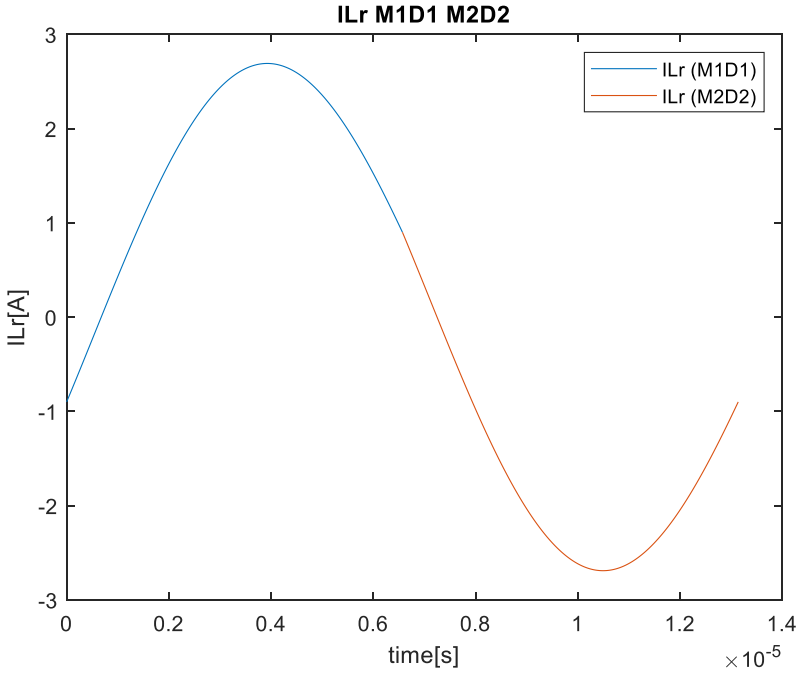

Figure 5. 6: current in Lr (resonant current) during M1D1 (blue) and M2D2 (red)

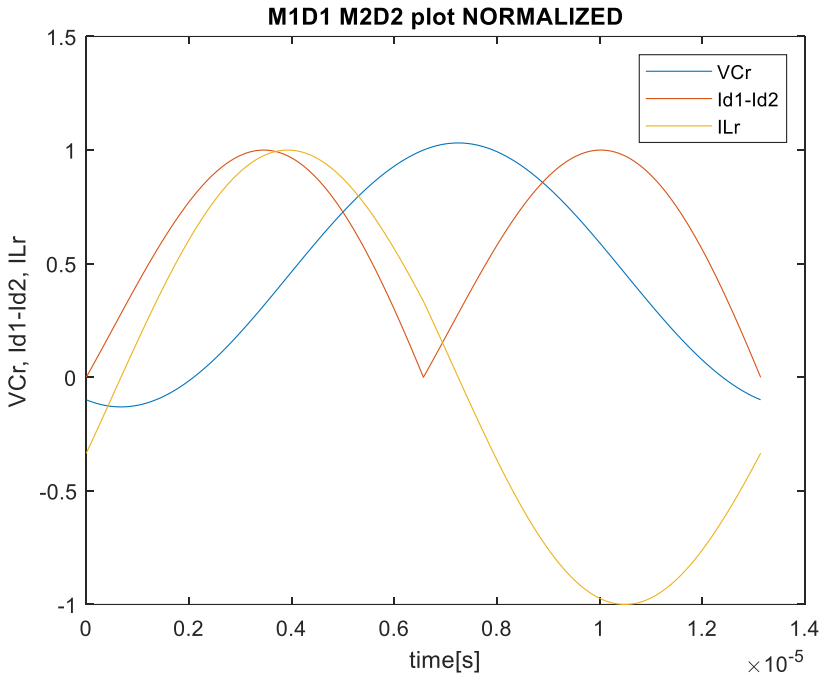

Figure 5. 7: VCr, Id1-Id2 and Ir during M1D1 and M2D2 normalized

5.3 Design at resonance for WPT with losses

The next step is to adapt the system for LLC converter with transformer for an LLC resonant converter for Wireless Power Transfer, that is an LLC with coupled inductors. The main issue that arises with coupled inductors is the lower number of degrees of freedom respect to the LLC with transformer. In fact, in an LLC with transformer, resonance inductance L_r is the inductance of a physical inductor, and it is not related to magnetizing inductance L_m and turn ratio n, which depend on the transformer. In an LLC with coupled inductors L_r, L_m and equivalent turn ratio (n_{eq}) all three depend on coupling coefficient k (which is dependent from the distance between the two coils). Remember the equations for the coupled inductors model:

$$L_m = k^2 \cdot L_1 \tag{5. 1}$$

$$L_r = (1 - k^2) \cdot L_1 \tag{5. 2}$$

$$n_{eq} = k \cdot \sqrt{\frac{L_1}{L_2}} = k \cdot \frac{N_1}{N_2} \tag{5. 3}$$

5. Design with steady-state switching sequence

If we suppose that the LLC converter works at resonance, the gain M is unitary and we can write:

$$\frac{2 \cdot n_{eq} \cdot V_{out}}{V_{in}} = 1$$

(5. 4)

In this case, n_{eq} is not given by N1/N2 (where N1 and N2 are the number of turns of the two coils) but it is the effective turn ratio given by equation 5.3, which depends on k. The resonance frequency, since depend on L_r, is also dependent on k:

$$f_r = \frac{1}{2\pi\sqrt{L_r C_r}}$$

(5. 5)

We can't follow the same approach used for the LLC with transformer. With coupled inductors, we must take into account the dependency on k. These are the preliminary steps of the new design method:

1. Start from fixed value of V_{in}, V_{out} and k
2. Compute the effective turn ratio n_{eq} from equation (5.4)
3. Compute L_r and L_m from L1 with (5.1) and (5.2)

Now we can use the previous MATLAB script (with some modifications) to find the optimal design for the LLC converter for WPT. In this case we also neglect the dead time T_D and study the evolution of two regions: M1D1 and M2D2. The optimizer tries to minimize the norm of the difference between two vectors of four elements, one contains the final values of the M2D2 region:

$$[V_{Cr}, I_{D2}, I_r, I_{out}]$$

And the desired initial conditions:

$$\left[V_{Cr\_0}, I_{D1\_0}, I_{r\_0}, V_{out}/R_{Load}\right]$$

But in this case, we have to change the parameters which the MATLAB optimizer varies, since we have the constrains due to the use of coupled inductors. In this case, the parameters that the optimizer can change are different from those of the previous case. They are the initial voltage across resonant capacitor V_{Cr}, the resonant capacitor C_r, the inductance of primary side coupled inductor (transmitter coil) and the effective turn ratio n_{eq}:

$$\left[V_{Cr}, C_r, L_1, n_{eq}\right]$$

Since the optimizer varies L_1, at the beginning of every system's evolution estimation (M1D1 - M2D2 cycle), the values of L_r and L_m must be updated (equations (5.1) and (5.2)). At the end of the process, we can compute the value L_2 from (5.3):

$$L_2 = L_1 \cdot \left(\frac{k}{n_{eq}}\right)^2 \qquad (5.6)$$

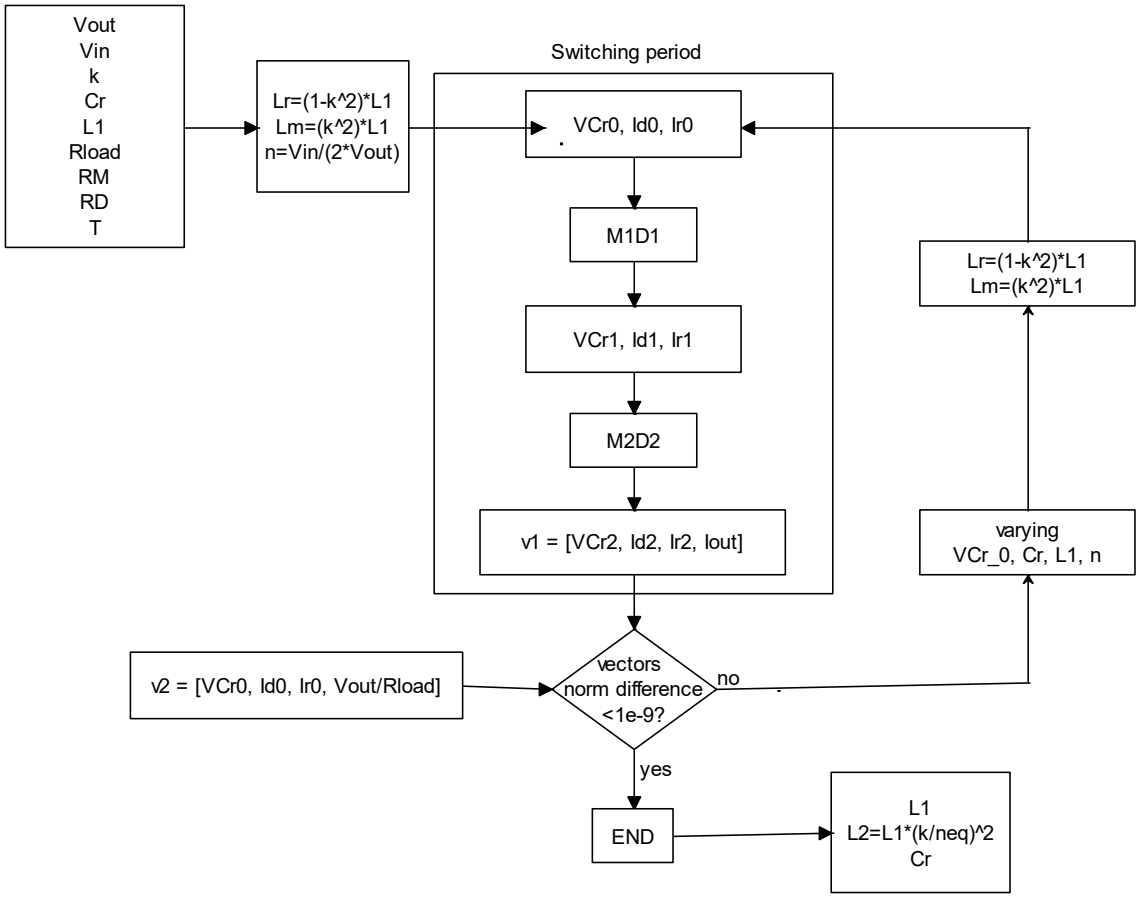

Figure 5. 8: design flow chart

5.4 Paper design

After the definition of the procedure to obtain an exact design for an LLC for Wireless Power Transfer, it was possible to do a comparison between the design described on a paper about the LLC for WPT [14] and the design obtained by the MATLAB script. The aim of the paper is to create a wireless charger for electric bicycles using the LLC resonant converter. A procedure to design a wireless LLC resonant converter for Wireless Power Transfer is described. In the paper the necessity to design at first the wireless transformer is highlighted as the priority parameter. In fact, resonant and magnetizing inductance depend on the transformer (witch in this case is wireless). The

battery to be charged is a lithium-ion battery 36V-2.9A. Since the input voltage to the converter is supposed to come from the main AC rectified and filtered, it is assumed to be 325V. The specifics are exhibited in the next table:

Input Voltage (V_{in})	325V
Output voltage range (V_{out})	36V÷ 40V
Output current (I_{out})	2.9A
Switching frequency (f_r)	200kHz

To ensure WPT, a 100x100 mm wireless transformer is used. The primary winding is 12x13 cm and the secondary is 10x10 cm.

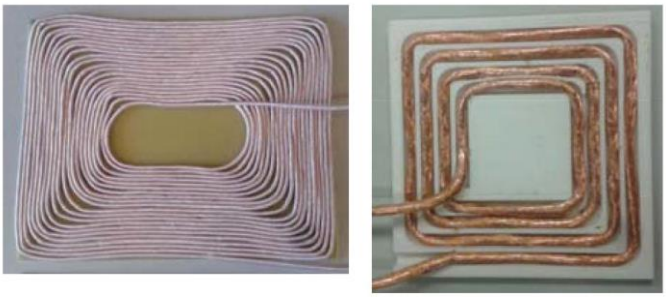

Figure 5. 9: coupled inductors

The transformer was characterized with an impedance analyser, according to the distance between the two windings. At the minimum distance (about 5mm) the leakage inductance is 45µH and the magnetizing inductance 30µH. The turn ratio of the transformer (N_1/N_2) is n=5. To have the resonant frequency at 200kHz, the capacitance of resonant capacitor can be derived from equation (5.5):

$$C_r = \frac{1}{(2 \cdot pi \cdot f_r)^2 \cdot L_r} = 14.07nF$$

(5. 7)

The LLC circuit is modelled with FHA, so the LLC converter is supposed to work at resonance. This means that switching frequency is equal to the resonant frequency ($f_{sw} = f_r$). Through FHA, the output voltage can be derived from the equation (2.18):

$$V_{out} = \frac{V_{in}}{2 \cdot n} = \frac{325V}{2 \cdot 5} = 32.5V$$

(5. 8)

This result doesn't match with the specifics (V_{out} = 36V - 40V). The first reason is that n=5 is the normal turn ratio (N1/N2), but the effective turn ratio to be considered in expression (5.8) should be the normal turn ratio multiplied for the coupling coefficient k of the coils (5.3). Since k is a fractional number between 0 and 1, the equivalent turn

ratio will be lower than normal turn ratio. Of consequence, output voltage will increase since it is inversely proportional to equivalent turn ratio. Another reason is that FHA is a strong approximated method which gives an ideal behaviour of the LLC converter. In a real circuit, the working region moves away from resonance and the frequency should be manually adjusted back to resonance. This is due to the non-idealities of the elements. At the end of the paper, the experimental results derived from a prototype for the verification of the theoretical computations are shown. To obtain an output voltage about 40V, the frequency is varied from 200kHz to 160kHz. This can be seen in figure 5.6, where the measured waveforms of the prototype are shown.

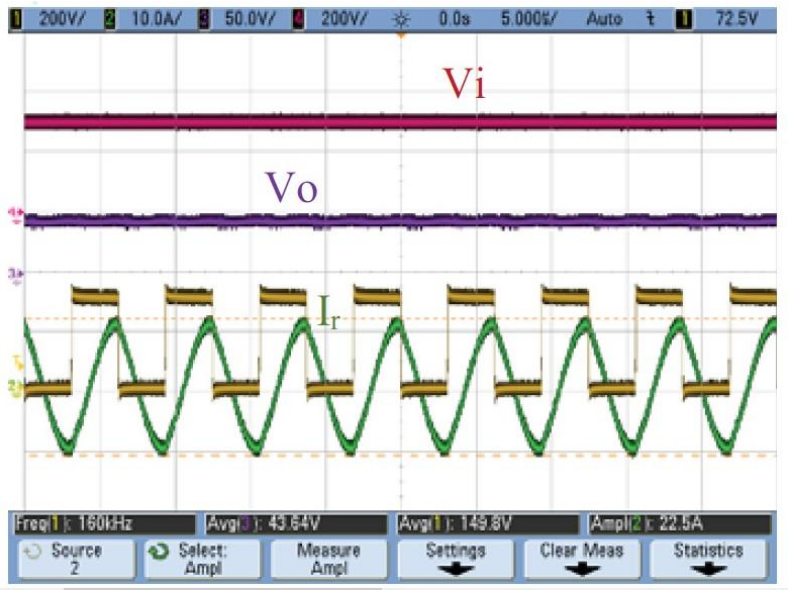

Figure 5. 10: LLC waveforms on the oscilloscope

The classic methods to design LLC (like FHA) do not consider the non-idealities (losses or forward diode voltages). So, the real circuit moves away from resonance. In order to return to resonance, the switching frequency is varied randomly. In fact, as in the case of this paper, the new resonance frequency moves to 160kHz. With the switching sequence method, an exact design (taking account of non-idealities) can be obtained for a fixed frequency.

5.4.1 Optimization of paper design (lossless)

The next step is to find the exact design for the specifics of the paper, which are:

- Input voltage: V_{in}
- Output voltage: V_{out}
- Coupled coefficient: k

5. Design with steady-state switching sequence

- Output current: I_{out}
- Load resistance: R_{load}
- Switching frequency: f_{sw}

At the beginning, we suppose that there are no losses. These specifics can be obtained by varying the resonant capacitor, the inductors and the equivalent turn ratio (the wireless transformer parameters) of the LLC circuit. Input voltage, output current and switching frequency are the same as before (V_{in}=325V, I_{out}=2.9A, f_{sw}=200kHz). Output voltage can be included between 36V and 40V. Now we choose a fixed value: V_{out}=40V. The reason behind choosing the upper limit of range is because an LLC converter for WPT is easier to be designed for higher values of output voltage. The next step is to compute the coupling coefficient k. This is possible by equation 5.1 and 5.2. From L_r and L_m, it is possible compute L_1 (which is the sum of L_r and L_m) and k as:

$$k = \frac{1}{\sqrt{\frac{L_r}{L_m} + 1}} \approx 0.63$$

(5. 9)

$$L_1 = L_r + L_m = 45\mu H + 30\mu H = 75\mu H$$

(5. 10)

At the end, the load resistance can be computed from output voltage and current:

$$R_{load} = \frac{V_{out}}{I_{out}} = \frac{40V}{2.9A} = 13.8\Omega$$

(5. 11)

Table with specifics:

Input voltage (V_{in})	325V
Output voltage (V_{out})	40V
Coupling coefficient (k)	0.63
Output current (I_{out})	2.9A
Load resistance (R_{load})	13.8Ω
Switching frequency (f_r)	200kHz

The first step is the simulation on LTspice of the LLC circuit with the specifics of the paper, to understand how the circuit works. In figure 5.11 the LTspice circuit is illustrated.

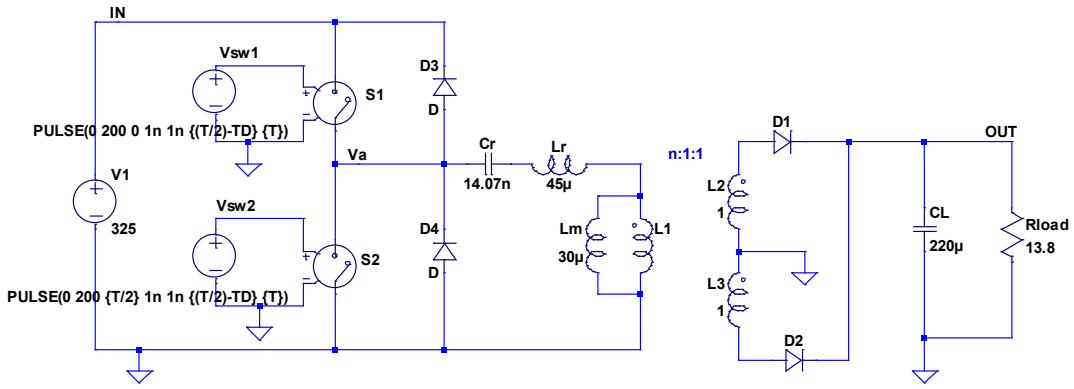

Figure 5. 11: LLC circuit in LTspice

In figure 5.12 there are the plots of main waveforms of LLC circuit.

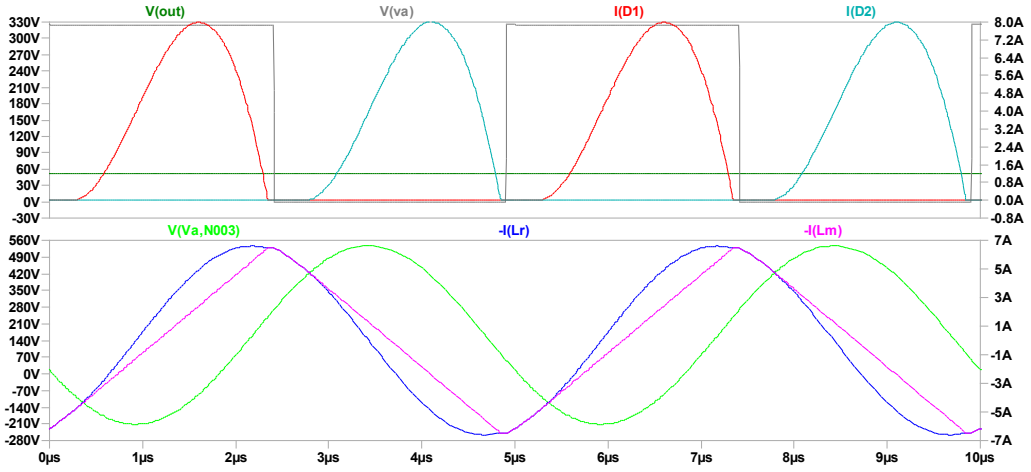

Figure 5. 12: LTspice waveforms of LLC converter

How it's possible to see from the plots, the diodes' current is discontinuous (DCM). There are some instants in which there is no current flowing in the secondary side. In fact, in these instants, the resonant current I(L_r) flows only in the magnetising inductance L_m and not into the primary side of the ideal transformer (I(L_r) = I(L_m)). This is due to the low value of magnetizing inductance and to a high value of load resistance. In fact, decreasing R_{load} at low value (2 Ohms) the diodes' current become continuous. From figure 5.12 it's clear that the circuit is not working at resonance. Moreover, the output voltage is about 50V since the turn ratio must be multiplied for the coupling coefficient, obtaining the equivalent turn ratio:

$$V_{out} = \frac{V_{in}}{2 \cdot (n \cdot 0.63)} = \frac{325V}{2 \cdot 3.15} \approx 52V \qquad (5.\ 12)$$

To find the exact design which meets the specifications, a MATLAB script which implements the switching sequence was used. The three starting conditions of the system are taken from the LTspice simulation:

- Voltage across resonant capacitor (initial value): V_{Cr0} = 16V
- Diode current (initial value): I_{D0} = 0A
- Resonant current (initial value): I_{Lr0} = -6A

The optimizer is able to minimize the norm under the threshold. But plotting the evolution of the systems (figure 5.13), diodes' current has not a correct behaviour since there are some instants in which it is negative.

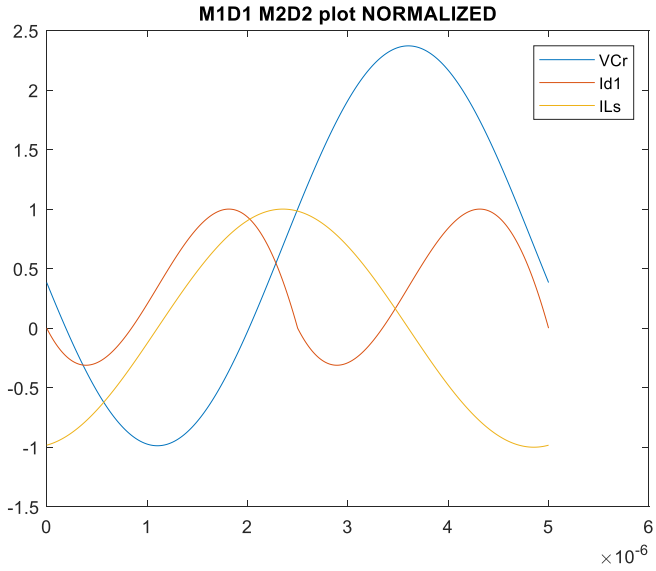

Figure 5. 13: Matlab plot

The problem is that the initial value of resonant current (-6A) is too high. This value must be higher than $-I_{ZVS}$, which is the minimum value of current to ensure Zero-Volt-Switching. This is the current which discharges the capacitor on node A. Furthermore, the absolute value of this current must not be too much low. A reasonable value is -0.9A. So, now the iteration will be repeated with the sequent initial values:

- V_{Cr0} = 16V
- iD_0 = 0A
- iL_{r0} = -0.9A

Now the optimizer still minimizes the norm under the threshold, and the diodes' current is continuous (CCM) and the voltage and current signals are sinusoidal (figure 5.14). The MATLAB script is exhibited in Appendix M.3.

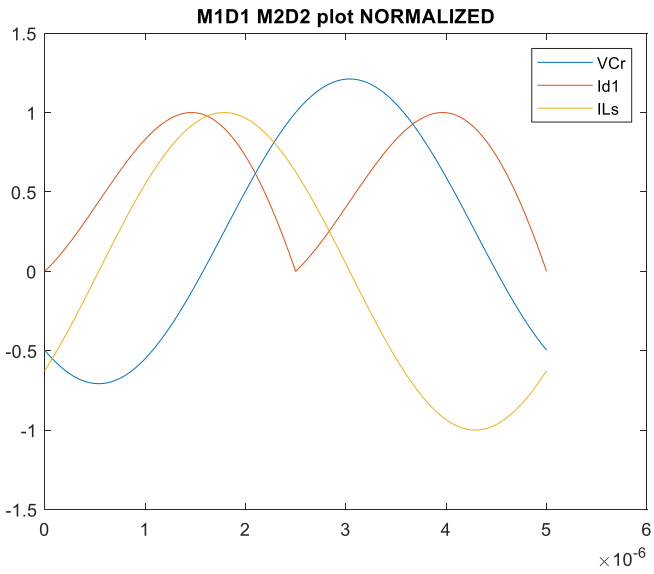

Figure 5. 14: Matlab plot

Values optimized on MATLAB:

V_{Cr0}	-320 V
C_r	1.84 nF
n_{eq}	4.0624
L_r	343 µH
L_m	226 µH
L_1	569 µH
L_2	13.5 µH

The values of leakage and magnetizing inductance are increased respect to the values of the paper (45uH and 30uH). In figure 5.15 there is the plot of LTspice simulations with the value of circuit elements obtained on MATLAB. The output voltage is about 39V.

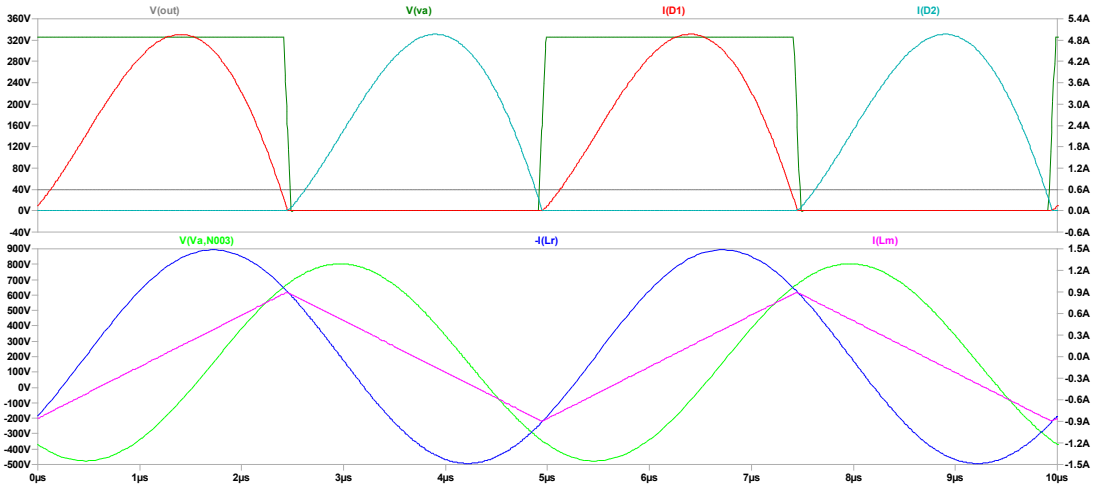

Figure 5. 15: LTspice waveforms of LLC for WPT optimized

5.4.2 Optimization of paper design with losses

The next step is to also consider the non-idealities of the circuit elements. These are the resistance of the components (the losses of MOSFET, diodes, capacitor and inductors) and the forward voltage of diodes. These are the values chosen for these three non-idealities:

- Total resistance on primary: RM=2Ω
- Total resistance on secondary: RD=0.5Ω
- Forward voltage diodes on secondary: 0.7V

After a parameter optimization on MATLAB, the new values are the following:

V_{Cr0}	-342 V
C_r	1.91 nF
n_{eq}	3.74
L_r	332 µH
L_m	219 µH
L_1	551 µH
L_2	15.6 µH

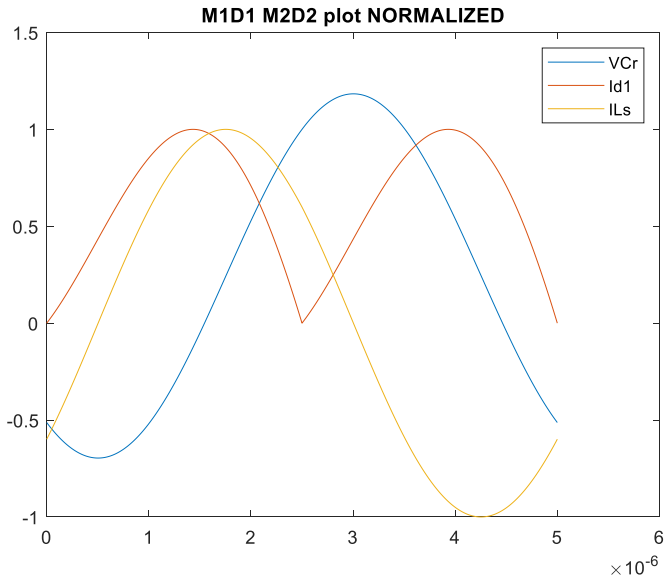

Figure 5. 16: Matlab plot

From LTspice simulation, Vout is about 40V, and the efficiency is about 92%. The efficiency is not high, but it is a good value considering the losses. Notice that the effective turn ratio is 3.74 (in the lossless case it was about 4).

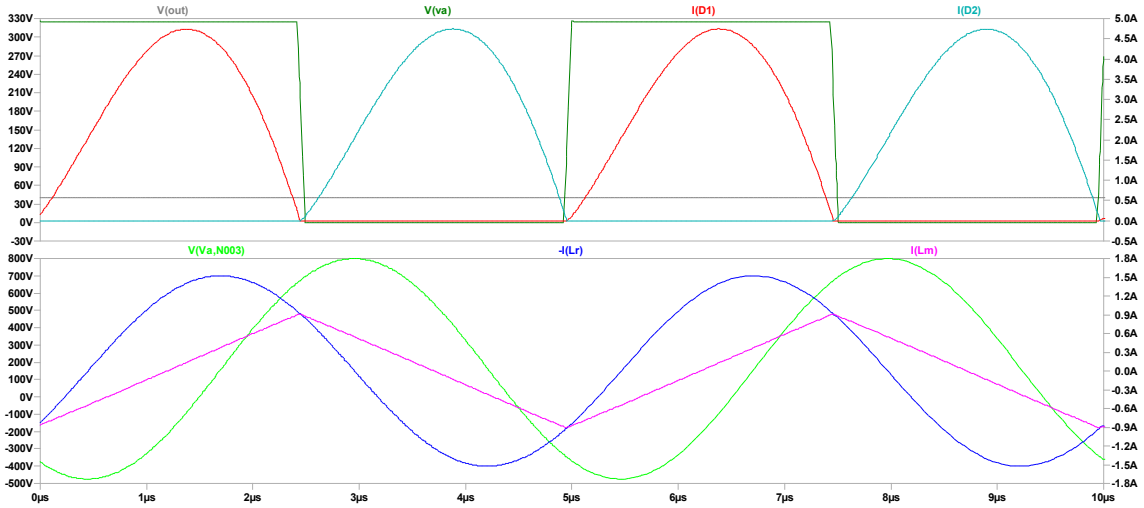

Figure 5. 17: : LTspice waveforms of LLC for WPT lossy optimized

5.4.3 Simulation varying the load

In this section the results of a simulation by varying the load resistance of 25% are shown. The simulation on LTspice demonstrates that the circuit works properly also with a load variation. Diodes' current is continuous and output voltage is about 40V. Output current decreases since the load is increased. The efficiency is about 93%.

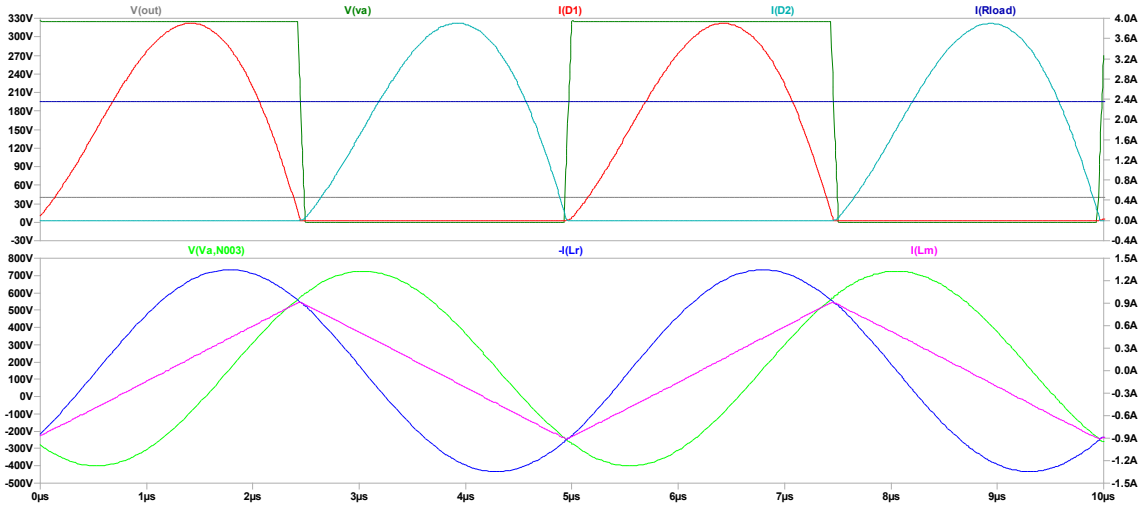

Figure 5. 18: LTspice waveforms of LLC for WPT with varied load

5.5 Normalized design

In this section the circuit parameters are normalized before the optimization on MATLAB. These are the normalizations of the circuit parameters:

- $C_{r,norm} = \frac{C_r \cdot \omega \cdot V_{in}^2}{V_{out} \cdot I_{out}}$
- $L_{1,norm} = \frac{L_1 \cdot \omega \cdot V_{in} \cdot I_{out}}{V_{in}^2}$
- $L_{r,norm} = \frac{L_r \cdot \omega \cdot V_{in} \cdot I_{out}}{V_{in}^2}$
- $L_{m,norm} = \frac{L_p \cdot \omega \cdot V_{in} \cdot I_{out}}{V_{in}^2}$
- $n_{eff,norm} = \frac{n_{eff} \cdot V_{out}}{V_{in}}$
- $V_{D1on,norm} = \frac{V_{D1,on}}{V_{out}}$, $V_{D2on,norm} = \frac{V_{D2,on}}{V_{out}}$
- $RM_{norm} = \frac{RM \cdot V_{out} \cdot I_{out}}{V_{in}^2}$
- $RD_{norm} = \frac{RD \cdot I_{out}}{V_{out}}$
- $V_{Cr0,norm} = \frac{V_{Cr0}}{V_{in}}$
- $I_{D1,norm} = \frac{I_{D1,on}}{I_{out}}$, $I_{D2,norm} = \frac{I_{D2,on}}{I_{out}}$
- $I_{Lr0,norm} = \frac{I_{Lr0} \cdot V_{in}}{V_{out} \cdot I_{out}}$

In figure 5.19 there is the plot of the waveforms on the circuit normalized and optimized.

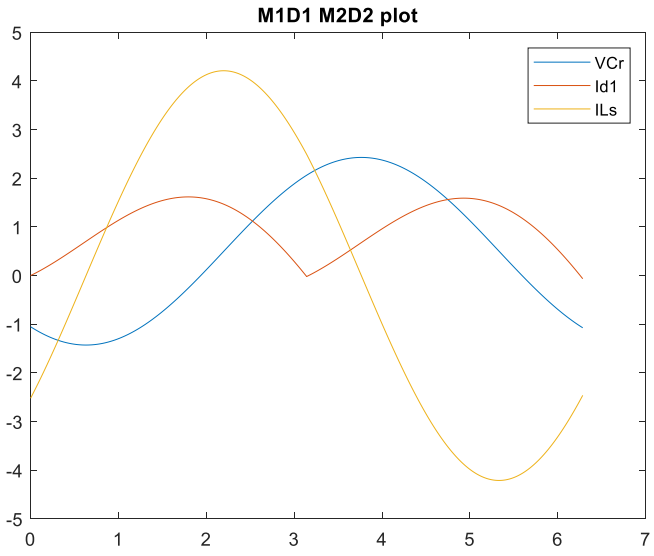

Figure 5. 19: Matlab plot

5.6 Varying switching frequency

To increase power density, switching frequency can be increased in order to reduce the dimension of reactive elements, in particular inductors. For the design of an LLC circuit with the values of leakage and magnetising inductance as in the paper (45µH and 30µH), we can vary the switching frequency and keeping constant the value of the resonant capacitor. The first step is to compute the ratio between the leakage inductance optimized on MATLAB and leakage inductance of the paper.

$$\frac{332\mu H}{45\mu H} = 7.4$$

(5. 13)

From the expression of resonant frequency, the new switching frequency will be:

$$f_{sw} = 200kHz \cdot \sqrt{7.4} = 540kHz$$

(5. 14)

MATLAB script moves the frequency to 577kHz and the resonant capacitor to 1.67nF. In figure 5.20 there are the plots of LTspice simulations.

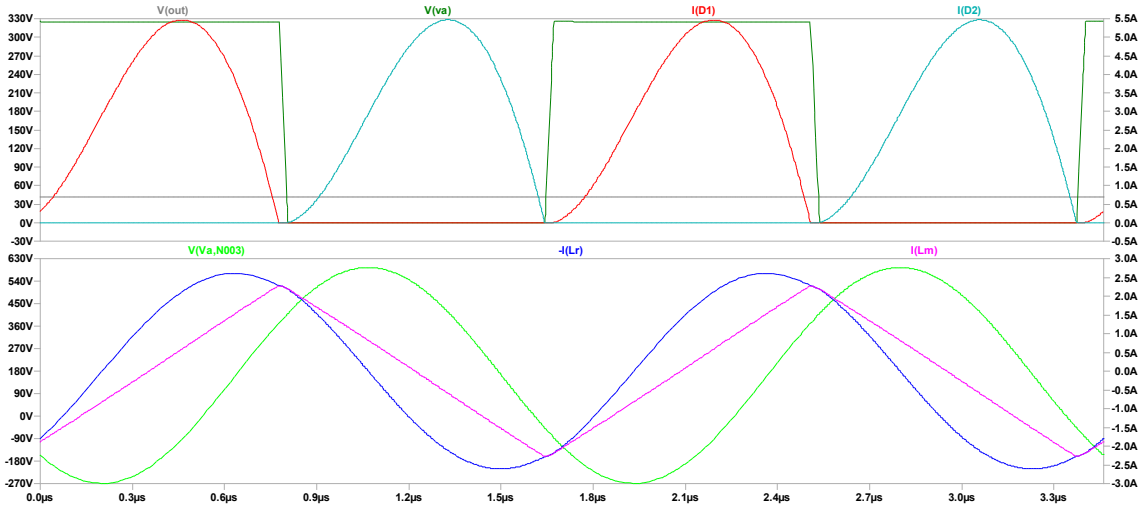

Figure 5. 20: LTspice waveforms of LLC for WPT

Conclusions

The aim of this thesis was the design progress for the LLC resonant converter for Wireless Power Transfer. First, the FHA approach was explained. This is the most applied technique, but it permits to obtain only an approximated design of the LLC. Then, the limits and problems due to the use of coupled inductors in the LLC converter was highlighted. Finally, a semi-analytical design was developed in order to obtain an exact design of the LLC for WPT, considering also the non-idealities. This design was obtained implementing the switching sequence technique by means of MATLAB scripts. MATLAB results have been verified to be in agreement with LTspice simulations. Furthermore, a comparison with the design of an LLC for WPT of a paper in the literature was made. The results obtained with MATLAB increase the values of the inductances of the paper in order to have a circuit which works at resonance with the same specifications of the paper. The LTspice simulations demonstrate that the circuit works properly even if the load varies of 25%. In conclusion, it was shown how to improve the power density by decreasing the values of the inductors and increasing the switching frequency, still making the circuit working at resonance. The results obtained in this thesis could be used for future studies about the LLC for WPT, for example to design the PCB layout for a prototype of the circuit or to find the design of the LLC when it is not working at resonance.

Appendix of Matlab scripts

M.1 design with FHA

```
%%%%%%%%%%%%%%%%%%%%%%% SPECIFICS %%%%%%%%%%%%%%%%%%%%%%%
global Q_ZVS
Vdc_min = 320; % Input voltage range
Vdc_Max = 420;
Vin_nom = 390; % Nominal input voltage
% Output Voltage:
% -Vout = 200V --> Iout = 1.6A
% -Vout = 75V --> Iout = 1A
Vout = 200; %Regulated output voltage 200
Iout = 1.6; %Regulated output current 1.6
Pout = Vout*Iout; % Maximum output power
perc = 0.95;
fr = 120e+3; % Resonant frequency
fr_Max = 150e+3; % Maximum operating frequency
% Compute Rload as avarage of resistances for
% the two possible Vout (200V(1.6A)-75V(1A))
Rload =((200/1.6)+(75/1))/2; % --> 100
TD = 270e-9; % Deadtime
C_ZVS = 350e-12; % Parasitic Capacitance at node N

%%%%%%%%%%%%%%%%%%%%%%% STEP 1 %%%%%%%%%%%%%%%%%%%%%%%
% Gain at nominal input voltage is 1
n = (1/2)*(Vin_nom/Vout) % Transformer Turn Ratio. At fr
                         % the Gain is 1 -> M = (2*n*Vout/Vin) = 1

%%%%%%%%%%%%%%%%%%%%%%% STEP 2 %%%%%%%%%%%%%%%%%%%%%%%
% Max. and min. required gain at the extreme values of the input
% voltage range
M_Max = 2*n*Vout/Vdc_min
M_min = 2*n*Vout/Vdc_Max

%%%%%%%%%%%%%%%%%%%%%%% STEP 3 %%%%%%%%%%%%%%%%%%%%%%%
% Maximum normalized operating frequency
fn_Max = fr_Max/fr

%%%%%%%%%%%%%%%%%%%%%%% STEP 4 %%%%%%%%%%%%%%%%%%%%%%%
%Effective load resistance reflected at transformer primary side (FHA)
Rac = (8/pi^2)*(n^2)*(Rload) % Rac = (8/pi^2)*(n^2)*(Vout^2/Pout);

%%%%%%%%%%%%%%%%%%%%%%% STEP 5 %%%%%%%%%%%%%%%%%%%%%%%
% Impose that the converter operates at maximum frequency at zero
% load (Q=0) and maximum input voltage (M_min)
% Calculate the inductance ratio lambda=Lr/Lm = 1/lm
lambda = ((1-M_min)/M_min)*(fn_Max^2)/(fn_Max^2 - 1);

%%%%%%%%%%%%%%%%%%%%%%% STEP 6 %%%%%%%%%%%%%%%%%%%%%%%
% Max Q value to work in the ZVS operating region at minimum input
% voltage (M_Max) and full load condition
Q_Max = (lambda/M_Max)*sqrt(1/lambda + (M_Max^2)/(M_Max^2 - 1));
Q_ZVS_1 = perc*Q_Max % perc = 95%
```

```
%%%%%%%%%%%%%%%%%%%%%%% STEP 7 %%%%%%%%%%%%%%%%%%%%%%%
% Max Q value to work in the ZVS operating region at no-load
% condition and maximum input voltage
Q_ZVS_2 = (2/pi)*(lambda*fn_Max/((lambda + 1)*fn_Max^2 -
lambda))*TD/(Rac*C_ZVS)

%%%%%%%%%%%%%%%%%%%%%%% STEP 8 %%%%%%%%%%%%%%%%%%%%%%%
% Max quality factor for ZVS in the whole operating range
Q_ZVS = min([Q_ZVS_1 Q_ZVS_2]); % Q_ZVS <= min{Q_ZVS1, Q_ZVS2};

%%%%%%%%%%%%%%%%%%%%%%% STEP 9 %%%%%%%%%%%%%%%%%%%%%%%
% Minimum operating frequency at full load and minimum input voltage
f_min = fr*sqrt(1/(1 + (1/lambda)*(1 - 1/power(M_Max,1 +
(Q_ZVS/Q_Max)^4))));
fn_min = f_min/fr;

%%%%%% Iterations for ZVS %%%%%
% normalized input impedance
Zn = 1j*fn_min/(lambda + 1j*fn_min*Q_ZVS) + (1 -
fn_min^2)/(1j*fn_min);
% Condition for ZVS: imag(Zn)/real(Zn) >= %
C_ZVS*(Vdc_min^2)/(pi*TD*Pout)
y = imag(Zn)/real(Zn) - C_ZVS*(Vdc_min^2)/(pi*TD*Pout);
while y<0.1 % margin of 0.1
    global Q_ZVS
    perc = perc-0.01;
    Q_ZVS_1 = perc*Q_Max;
    Q_ZVS = min([Q_ZVS_1 Q_ZVS_2]); % Q_ZVS <= min{Q_ZVS1, Q_ZVS2};
    f_min = fr*sqrt(1/(1 + (1/lambda)*(1 - 1/power(M_Max,1 +
(Q_ZVS/Q_Max)^4))));
    fn_min = f_min/fr;
    Zn = 1j*fn_min/(lambda + 1j*fn_min*Q_ZVS) + (1 -
fn_min^2)/(1j*fn_min);
    y = imag(Zn)/real(Zn) - C_ZVS*(Vdc_min^2)/(pi*TD*Pout);
end

%%%%%%%%%%%%%%%%%%%%%%% STEP 10 %%%%%%%%%%%%%%%%%%%%%%%
% Characteristic impedance of the resonant tank and
% all components values
final_Q_ZVS_1 = Q_ZVS_1

Zo = Q_ZVS*Rac % characteristic impedance
Cr = 1/(2*pi*fr*Zo)
Lr = Zo/(2*pi*fr)
Lm = Lr/lambda
```

M.2 switching sequence design of LLC

```
% Specs and Initial Condition
% if variables have subscript _0 e.g. x_0 means initial condition

% initial state variables condition condition
VCr_0 = -43.954350445525151;
id1_0 = 0;
iLs_0 = -0.9; % derived from discharge parasitics cap in dead time
              % Ils=Cpar*(Vin)/Tdead
```

```
global Ls Vin VD1_on VD2_on VBD_on Vout Td C1 C2 R_M R_D Cr

Ls = 200e-6; % Ls = Lr
Cr = 22e-9;
Lp_0 = 712.4787515538974e-6; % Lp = Lm
Vin = 399.84;
VD1_on = 0;
VD2_on = 0;
VBD_on = 0;
Vout = 24;
a_0 = 7.727511612852854; % a = n (turn ratio)
T_0 = 1.313853966821311e-05;
format long
freq=1/T_0
Td = 90e-9;
C1 = 100e-12;
C2 = 100e-12;

RL=1.9; %load resistance

R_M = 1;
R_D = 0.1;

% Optimization

options =
optimset('Display','iter','PlotFcns',@optimplotfval,'TolFun',1e-
9,'MaxFunEvals',2500);

tic
fToMinimize = @(x) norm(end_cond_finder(x(1),id1_0, iLs_0, x(2),
x(3),x(4))-[x(1), id1_0, iLs_0, Vout/RL]);
% output vector
[R,fval,exitflag,output] =
fminsearch(fToMinimize,[VCr_0,a_0,Lp_0,T_0],options);
toc

% R is the vector containing the results
format long
VCr_0=R(1)
a_0=R(2)
Lp_0=R(3)
T_0=R(4)
freq=1/T_0

% function definition
function y = end_cond_finder(VCr_0,id1_0,iLs_0,a,Lp,T)

global Ls Vin VD1_on VD2_on VBD_on Vout Td C1 C2 R_M R_D Cr

% M1D1

A_M1D1 = [        0,                                    0,        1/Cr;
 -a/Ls, -(a*(Lp*R_D*a + Ls*R_D*a))/(Lp*Ls), -(R_M*a)/Ls;
 -1/Ls,                         -(R_D*a)/Ls,     -R_M/Ls];
```

```
b_M1D1 = [                                                                  0;
-(a*(Lp*VD1_on*a-Lp*Vin+Ls*VD1_on*a + Lp*Vout*a + Ls*Vout*a))/(Lp*Ls);
                                        -(VD1_on*a - Vin + Vout*a)/Ls];

%initial conditions
x_0 = [VCr_0 id1_0 iLs_0];
% ode45
T1 = linspace(0,T/2,1000);
ops = odeset('RelTol',1e-10,'AbsTol',1e-10);
f_M1D1=@(x) A_M1D1*x + b_M1D1;
[T1,x1] = ode45(@(t,x1) f_M1D1(x1), T1, x_0,ops);

% M2D2

A_M2D2 = [      0,                                      0,       1/Cr;
  a/Ls, -(a*(Lp*R_D*a + Ls*R_D*a))/(Lp*Ls), (R_M*a)/Ls;
 -1/Ls,                          (R_D*a)/Ls,    -R_M/Ls];

b_M2D2 = [                                                              0;
 -(a*(Lp*VD2_on*a + Ls*VD2_on*a + Lp*Vout*a + Ls*Vout*a))/(Lp*Ls);
                                          (VD2_on*a + Vout*a)/Ls];

Vcr_2 = x1(end,1);
id2_2 = 0;
iLs_2 = x1(end,3);
x_2=[Vcr_2 id2_2 iLs_2];

T2 = linspace(0,T/2,1000);

f_M2D2=@(x) A_M2D2*x + b_M2D2;
[T2,x2] = ode45(@(t,x2) f_M2D2(x2), T2, x_2,ops);

y(1) = x2(end,1); % VCr
y(2) = x2(end,2); % Id
y(3) = x2(end,3); % Ir
y(4) = (trapz(T1,x1(:,2)) + trapz(T2,x2(:,2)))/T; %  mean(Id1)=Vout/RL
```

M.3 switching sequence design of LLC for WPT

```
% Specs and Initial Condition
% if variables have subscript _0 e.g. x_0 means initial condition
% initial state variables condition condition
VCr_0 = -342.0088500396224;
id1_0 = 0; % 0
iLs_0 = -0.9; % derived from discharge parasitics cap in dead
              % Ils=Cpar*(Vin)/Tdead

global Vin VD1_on VD2_on VBD_on Td C1 C2 R_M R_D  k Vout
Vin = 325;
Vout = 40;
% FHA (Firts Harmonic Approximation)
% Transfer Function at Resonance (fsw = fr): Vout = Vin/(2*a)
% Resonance Frequency: fr = 1/(2*pi*sqrt(Lr*Cr))
% We derive a_0 (effective turn ratio) by FHA
a_0 = Vin/(2*Vout); % a = effective Turn Ratio, --> 4.0625
```

```
% a_0 = 3.740533391492024; % optimized value
k = 0.63; % Coupling factor
L1 = 551.7089961876713e-6;
Ls = (1-k^2)*L1; % Serie Inductor (Lr)
Lp_0 = (k^2)*L1; % Parallel Inductor (Lm)
% NOTE: ratio Ls/Lp shoupld be 1.5
Cr = 1.914052073148292e-09;
f_r = 1/(2*pi*sqrt(Ls*Cr)) % resonance frequency
fsw=200e+3;
T_0 = 1/fsw; % f = 200kHz
format long

Td = 90e-9;
C1 = 100e-12;
C2 = 100e-12;
VD1_on = 0.7;
VD2_on = 0.7;
VBD_on = 0;

% Iout = 2.9A --> Rout = Vout/Iout = 13.8 Ohm
RL=13.8; %load resistance

R_D = 0.5;
R_M = 2;

% Optimization problem
close all;
options =
optimset('Display','iter','PlotFcns',@optimplotfval,'TolFun',1e-
9,'MaxFunEvals',2500);

tic
fToMinimize = @(x) norm(end_cond_finder(x(1),id1_0, iLs_0, x(2), x(3),
T_0, x(4))-[x(1), id1_0, iLs_0, Vout/RL]);
% output vector
[R,fval,exitflag,output] =
fminsearch(fToMinimize,[VCr_0,Cr,L1,a_0],options);
toc

% R is the vector containing the results
format long
VCr_0=R(1)
Cr=R(2)
L1=R(3)
a_0=R(4)

N12 = (a_0/k)^2; % -> N12 = L1/L2, a=k*sqrt(L1/L2),
L2 = L1/N12 % Secondary Coil
Ls = (1-k^2)*L1 % Serie Inductor (Lr)
Lp_0 = (k^2)*L1 % Parallel Inductor (Lm)
f_r = 1/(2*pi*sqrt(Ls*Cr)) % resonance frequency

% function definition
function y = end_cond_finder(VCr_0,id1_0,iLs_0,Cr,L1,T,a)

global Vin VD1_on VD2_on VBD_on  Td C1 C2 R_M R_D k Vout

Ls = (1-k^2)*L1; % Serie Inductor (Lr)
```

```
Lp = (k^2)*L1; % Parallel Inductor (Lm)

% M1D1
A_M1D1 = [        0,                                        0,        1/Cr;
 -a/Ls, -(a*(Lp*R_D*a + Ls*R_D*a))/(Lp*Ls), -(R_M*a)/Ls;
 -1/Ls,                          -(R_D*a)/Ls,     -R_M/Ls];

b_M1D1 = [                                                                  0;
-(a*(Lp*VD1_on*a-Lp*Vin + Ls*VD1_on*a+Lp*Vout*a + Ls*Vout*a))/(Lp*Ls);
                                          -(VD1_on*a - Vin + Vout*a)/Ls];

%initial conditions
x_0 = [VCr_0 id1_0 iLs_0];
% ode45
T1 = linspace(0,T/2,1000);
ops = odeset('RelTol',1e-10,'AbsTol',1e-10);
f_M1D1=@(x) A_M1D1*x + b_M1D1;
[T1,x1] = ode45(@(t,x1) f_M1D1(x1), T1, x_0,ops);

% M2D2
A_M2D2 = [      0,                                      0,       1/Cr;
  a/Ls, -(a*(Lp*R_D*a + Ls*R_D*a))/(Lp*Ls), (R_M*a)/Ls;
 -1/Ls,                          (R_D*a)/Ls,    -R_M/Ls];

b_M2D2 = [                                                                  0;
    -(a*(Lp*VD2_on*a + Ls*VD2_on*a + Lp*Vout*a + Ls*Vout*a))/(Lp*Ls);
                                                (VD2_on*a + Vout*a)/Ls];

Vcr_2 = x1(end,1);
id2_2 = 0;
iLs_2 = x1(end,3);
x_2=[Vcr_2 id2_2 iLs_2];

T2 = linspace(0,T/2,1000);

f_M2D2=@(x) A_M2D2*x + b_M2D2;
[T2,x2] = ode45(@(t,x2) f_M2D2(x2), T2, x_2,ops);

y(1) = x2(end,1);
y(2) = x2(end,2);
y(3) = x2(end,3);
y(4) = (trapz(T1,x1(:,2)) + trapz(T2,x2(:,2)))/T; % mean(Id1)=Vout/RL
end
```

References

[1] A. Celentano et al., *A Comparison between Class-E DC-DC Design Methodologies for Wireless Power Transfer*, IEEE International Midwest Symposium on Circuits and Systems (MWSCAS), 2021

[2] A. Celentano et al., *A Wireless Power Transfer System for Biomedical Implants based on an isolated Class-E DC-DC Converter with Power Regulation Capability*, 2020 IEEE 63rd International Midwest Symposium on Circuits and Systems (MWSCAS), 2020

[3] T.-S. Chan, C.-L. Chen, *LLC Resonant Converter for Wireless Energy Transmission System with PLL Control*, 2008 IEEE International Conference on Sustainable Energy Technologies, 2008

[4] H. Ding, *Design of Resonant Half-Bridge converter using IRS2795(1,2) Control IC*, Application Note AN-1160, 2010

[5] A. Dumais, *LLC Resonant Converter Reference Design using the dsPIC® DSC*, Microchip WebSeminar, 2010

[6] G. Giorgino, *Analysis and design of half-bridge LLC resonant power converters*, Master's degree in Electronic Engineering (Politecnico di Torino), 2020

[7] H.-I. Hsieh, T.-H. Huang, S.-F. Shih, *An Inductive Wireless Charger for Electric Vehicle by using LLC Resonance with Matrix Ferrite Core Group*, IEEE Applied Power Electronics Conference and Exposition (APEC), 2015

[8] K. L. J. Kan, K.W.E. Cheng, *Design and Analysis of Mobile Near-Field Magnetic Power Transfer System with LLC Series Resonant Converter*, 8th International Conference on Power Electronics Systems and Applications (PESA), 2020

[9] T. Krigar, M. Pfost, *2-MHz Compact Wireless Power Transfer System With Voltage Conversion From 400V to 48V*, 2021 IEEE Wireless Power Transfer Conference (WPTC), 2021

[10] K. Naraharisetti, *Design of half bridge LLC resonant converter using synchronous rectifier*, 2015 IEEE International Conference on Electro/Information Technology (EIT), 2015

[11] On Semiconductor, *Basic Principles of LLC Resonant Half Bridge Converter and DC/Dynamic Circuit Simulation Examples*, Application Note AND9408/D, 2016

[12] On Semiconductor, *Half-Bridge LLC Resonant Converter Design Using FSFR-Series Fairchild Power Switch (FPS™)*, Application Note AN-4151, 2014

[13] Parimala S.K., M.S. Aspalli and L. Deshpande, *HIGH FREQUENCY DC-DC CONVERTER DESIGN USING ZERO VOLTAGE SWITCHING*, International Journal of Science, Environment and Technology, 2014

[14] A. M. Pernia et al., *Wireless LLC converter for electric bicycle*, 2020 IEEE Vehicle Power and Propulsion Conference (VPPC), 2020

[15] S. D. Simone, *LLC resonant half-bridge converter design guideline*, STMicroelectronics AN2450 Application note, 2014

[16] S.-T. Wu, C.-H. Han, *Design and Implementation of a Full-Bridge LLC Converter With Wireless Power Transfer for Dual Mode Output Load*, IEEE Access, 2021